ROW NUMBER EFFECT ON HEAT TRANSFER IN INLINE BANKS WITH FINNED TUBES

BY

XIYU YANG

Bachelor of Science

East China University of

Chemical Technology

Shanghai China

1990

Submitted to the Faculty of the
Graduate College of the
Oklahoma State University
in partial fulfillment of
the requirement for
the Degree of
MASTER OF SCIENCE
July, 1992

ROW NUMBER EFFECT ON HEAT TRANSFER

IN INLINE BANKS WITH

FINNED TUBES

Thesis Approved:

Kenneth J. Bell

Thesis Advisor

Arland H. Johannes

Alan Tree

Thomas C. Collins

Dean of the Graduate College

PREFACE

The row number effect on heat transfer for gases in cross flow over inline finned tube banks has been studied.

A two stream model was used to describe the air cross flow in the tube bank. One stream was the bypass stream which exists between the tips of fins of adjacent tubes, and it was assumed to give no heat transfer to or from the tube surface. The other was the primary stream which flows across the heat transfer surface and exchanges heat with the surface. An interchange stream existing between the bypass and primary streams. The heat transfer coefficient of the primary stream is treated as the actual heat transfer coefficient.

By using the two stream assumption, a mathematical model was developed to predict the air side temperature, row by row, and to reflect the row number effect on the apparent heat transfer coefficient.

I am very grateful to my adviser, Dr. K. J. Bell for his expert guidance and much valued counsel during the course of my study. I am also grateful to my Advisory Committee which consisted of Drs. A. H. Johannes and D. A. Tree, for their very helpful criticisms and suggestions.

I thank the School of Chemical Engineering of Oklahoma State University for providing me financial assistance

during the course of my study.

Finally, I would like to express my appreciation to my father, Mr. C. Yang and grandfather, Mr. Y. Wang for encouraging and providing me financial support through my education.

TABLE OF CONTENTS

LIST OF TABLES

LIST OF FIGURES

Figure | Page

NOMENCLATURE

A_0	Total outside surface area per unit length; ft^2/ft or m^2/m
$(A_f)_0$	Fin outside area per unit length; ft^2/ft or m^2/m
A_i	Tube inside area per unit length; ft^2/ft or m^2/m
A_{min}	Minimum flow area; ft^2 or m^2
A_{tot}	Total effective heat transfer surface area per row; ft^2/row or m^2/row
A_{ts}	Area of portion of tube sheets exposed to air flow; ft^2 or m^2
AMTD	Arithmetic mean temperature difference; ^0F or K (defined in Eq. 17)
C_n	Row correction factor ($C_n=Nu_n/Nu_\infty$); dimensionless
c_p	Heat capacity of fluid; Btu/(lbm-^0F) or kJ/(kg-K)
d_f	Fin outside diameter; ft or m
d_i	Tube inside diameter; ft or m
d_r	Tube root diameter; ft or m
G_{max}	Maximum stream mass velocity; lbm/(ft^2-sec) or kg/(m^2-sec)
H	Fin height; ft or m
h_a	Actual film heat transfer coefficient (based on the total outside surface area); Btu/(hr-ft^2-^0F) or W/(m^2-K)
h_{ap}	Actual film heat transfer coefficient for primary flow (based on the total outside surface area); Btu/(hr-ft^2-^0F) or W/(m^2-K)
h_c	Film heat transfer coefficient calculated assuming 100 percent fin efficiency (based on the total outside surface area); Btu/(hr-ft^2-^0F) or W/(m^2-K)

h_{cp} Film heat transfer coefficient calculated assuming 100 percent fin efficiency for primary flow (based on the total outside surface area); Btu/(hr-ft^2-^{0}F) or W/(m^2-K)

h_i Tube side heat transfer coefficient (based on the total outside effective heat transfer area); Btu/(hr-ft^2-^{0}F) or W/(m^2-K)

j Colburn factor (defined in Eq. 3); dimensionless

k Thermal conductivity; Btu/(hr-ft-^{0}F) or W/(m-K)

L Tube length; ft or m

l Fin height; ft or m

l_c Length of cut from fin tip; ft or m

l_e Effective fin height; ft or m

l_f Fin height; ft or m

LMTD Logarithmic mean temperature difference; ^{0}F or K (defined in Eq. 16)

M Total stream mass flow rate; lbm/hr or kg/s

MTD Mean temperature difference; ^{0}F or K (defined in Eq. 16 or 17)

m Individual stream mass flow rate; lbm/hr or kg/s

n Number of a given tube row in the tube bank ; dimensionless

n_s Number of fin segments per revolution;

n_f Fins per unit length; ft^{-1} or m^{-1}

N_t Number of tube rows or layers in the direction of flow

Nu Nusselt number (defined in Eq. 4); dimensionless

p Defined in Eq. 11; ft^{-1} or tube row^{-1}

Pr Prandtl number (defined in Eq. 2); dimensionless

p_l Longitudinal pitch; ft or m

p_t Transverse pitch; ft or m

Q Amount of heat transferred; Btu/hr or kJ/s

q Defined in Eq.12; ft^{-1} or tube row^{-1}

Re Reynolds Number (defined as Eq. 1); dimensionless

R_{th} Thermal resistance (tube side convective resistance and the tube wall conductive resistance); $(hr\text{-}ft^2\text{-}^0F)/Btu$ or $(hr\text{-}K)/W$

s Space between fins $(s=s_f-t_f)$; ft or m

s_f Fin spacing, center to center; ft or m

s_3 Longitudinal tube gap width; ft or m

T Stream temperature; ^0F or K

T_{in} Temperature of stream entering the tube bank; ^0F or K

$\bar{T}_{out}$ Average outlet stream temperature; ^0F or K

T_s Tube side stream temperature; ^0F or K

t_e Effective fin thickness; ft or m

t_f Fin thickness; ft or m

U_0 Overall heat transfer coefficient calculated using LMTD method and mixed stream terminal temperatures (based on total outside surface area); $Btu/(hr\text{-}ft^2\text{-}^0F)$ or $W/(m^2\text{-}K)$

U_p Overall heat transfer coefficient for primary stream (based on total outside surface area); $Btu/(hr\text{-}ft^2\text{-}^0F)$ or $W/(m^2\text{-}K)$

V Stream velocity; ft/sec or m/sec

V_{max} Maximum stream velocity; ft/sec or m/sec

W_b Bypass stream flow rate in the Bell and Kegler model; lbm/hr or kg/hr

W_p Primary stream flow rate in the Bell and Kegler model; lbm/hr or kg/hr

w_s Width of fin segment, serrated fin; ft or m

x Additional cross flow area due to non-ideal tube bank layout; ft^2 or m^2

Y Mean fin thickness; ft or m

m Fin efficiency parameter; ft^{-1} or m^{-1} (defined in Eq.6)

Greek:

α Defined in Eq. 13; ft^{-1} or tube row^{-1}

β Defined in Eq. 13; ft^{-1} or tube row^{-1}

γ Defined in Eq. 13; ft^{-1} or tube row^{-1}

μ Fluid viscosity; lbm/ft sec or N sec/m

ρ Fluid density; lbm/ft or kg/m

Ω Fin efficiency (defined in Eq. 5); dimensionless

Subscripts:

b Bypass stream

e Interchange stream

i Stream approaching a given tube row

n Number of the given tube row

o Stream exiting a tube row

p Primary flow

∞ Deep tube bank

CHAPTER I

INTRODUCTION

In many process and power plants, heat recovery equipment is designed with a gas stream in cross-flow across banks of finned tubes. The tube banks are arranged in inline or staggered layouts. An equilateral triangular tube arrangement is often used for staggered tube banks (see Figure 1a), and the inline tube banks often have a square

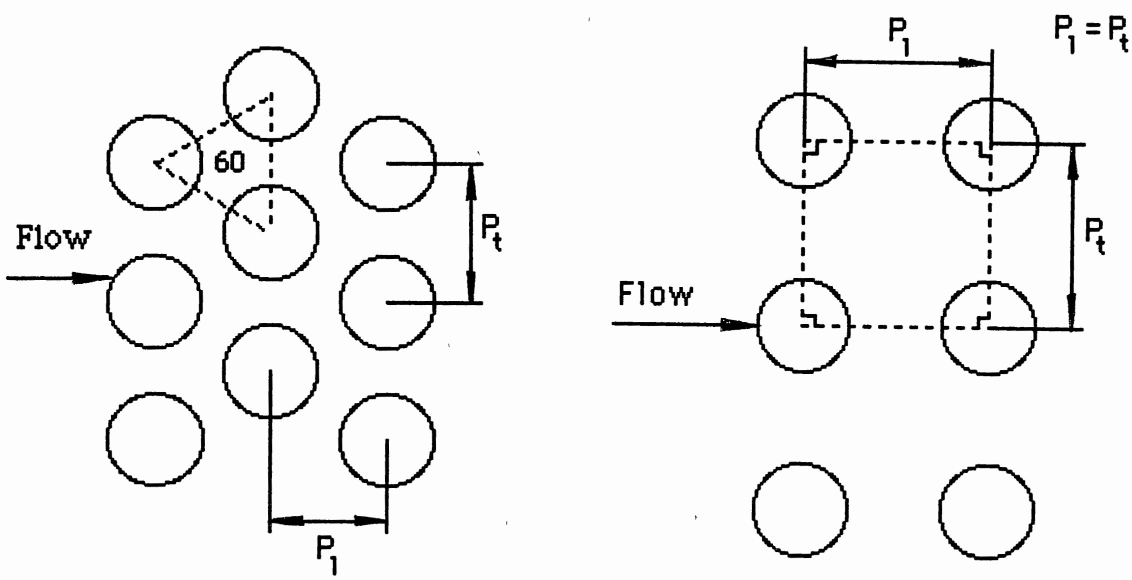

Staggered
(Equilateral Triangular Pitch)
(a)

Inline
(Square Pitch)
(b)

Figure 1. Tube Bank Layouts

tube arrangement (see Figure 1b). The longitudinal, p_l and transverse, p_t, pitches of staggered and inline tube banks are defined in Figure 1a and 1b. Because of the low heat transfer coefficient of the gas, it is desirable to use finned tubes to enlarge the heat transfer area and overall heat transfer rate. The fin geometries can be circular or rectangular, segmented or solid. The circular segmented fin is one of the most widely used geometries (see Figure 2). Some of the finned tube geometrical parameters (the tube root diameter d_r, fin outside diameter d_f, tube inside diameter d_i, fin segment width w_s and fin height l) are defined in Figure 2.

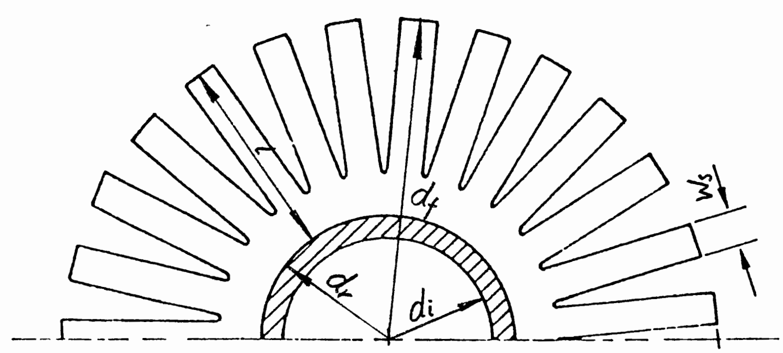

Figure 2. Segmented Fin Tube Geometry

For a finned tube bank, the Reynolds number is defined by

$$Re = G_{max} d_r / \mu. \tag{1}$$

The Prandtl number is defined by

$$Pr = \frac{c_p \mu}{k}. \tag{2}$$

The j factor is defined by

$$j = \frac{h_c}{G_{max} c_p} Pr^{2/3}. \tag{3}$$

The Nusselt number is defined by

$$Nu = \frac{h_c D_r}{k}. \tag{4}$$

Both the j factor and the Nusselt number are functions of the Reynolds number and the Prandtl number.

The finned tube is used to increase the heat transfer rate by increasing the heat transfer area. But the thermal resistance due to the heat transfer through the length of the fin needs to be considered. The fin efficiency concept is a common one used to account for the thermal resistance. The fin efficiency is defined as the amount of heat the fin actually transfers divided by the amount of heat it would transfer if the thermal conductivity of the fin metal were infinite. An idealized analysis gives:

$$\Omega = \frac{\tanh(z l_e)}{(z l_e)} \tag{5}$$

where

$$z = \sqrt{\frac{2h_c}{kt_e}} \quad ; \quad t_e = \frac{t_f w_s}{t_f + w_s} \quad ; \quad l_e = l \qquad (6)$$

from Weierman and Taborek (1978).

The inline finned tube bank is used because it can be cleaned with commercially available on-line soot-blowing methods. However, there is a strong row number effect on the heat transfer for the inline tube bank. The thermal performance of a deep inline tube bank (greater than about 10 or 12 tube rows deep) is close to that of a staggered tube bank. But, for a shallow tube bank, the inline tube bank shows a significantly decreased heat transfer coefficient when the data are interpreted by the simple LMTD method. (Note: In this paper, the heat transfer coefficient refers to that calculated by the LMTD method without further definition.) Also, the longitudinal tube pitch can affect the thermal performance of the inline tube bank.

Bell and Kegler (1978) made a mathematical analysis of the effect of flow bypass on the performance of an inline heat exchanger. They divided the flow in the inline tube bank into two parts: primary flow and bypass flow. (see Figure 3) Their model shows that the LMTD method is not valid if a bypass flow exists.

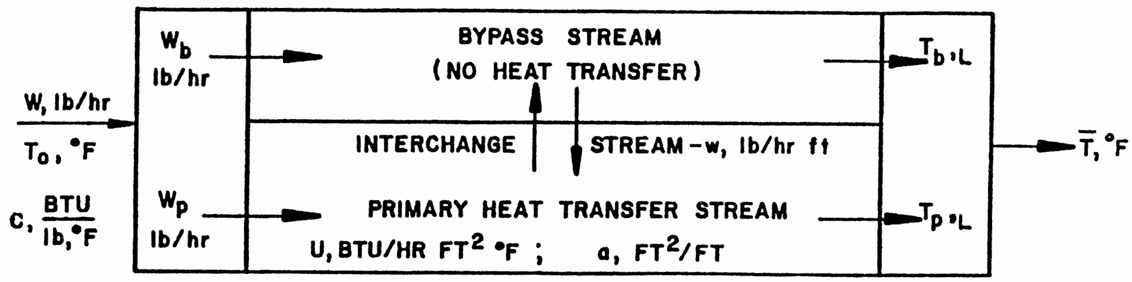

Figure 3. Thermal Analysis of the Bell and Kegler Model (1978)

This thesis modifies Bell and Kegler's model and generalizes it. With some further assumptions, the flows in inline tube bank are re-defined like those in Figure 4. In this thesis, I attempt to explain that the row number effect in shallow inline tube banks mainly results from the increasing interchange flow rate at these tube rows. The interchange flow exists between the bypass and primary flows and appears to vary from row to row among the first several tube rows, and then to approach a constant value. This results in the heat transfer coefficient for shallow inline tube banks having an obvious row number dependence, while the coefficient for the deep tube bank does not. The heat transfer coefficient increases with the increasing number of tube rows in the shallow tube bank, but remains constant in the deep tube bank. This is also the main reason that the shallow inline tube banks have lower heat transfer coefficients than deep tube banks.

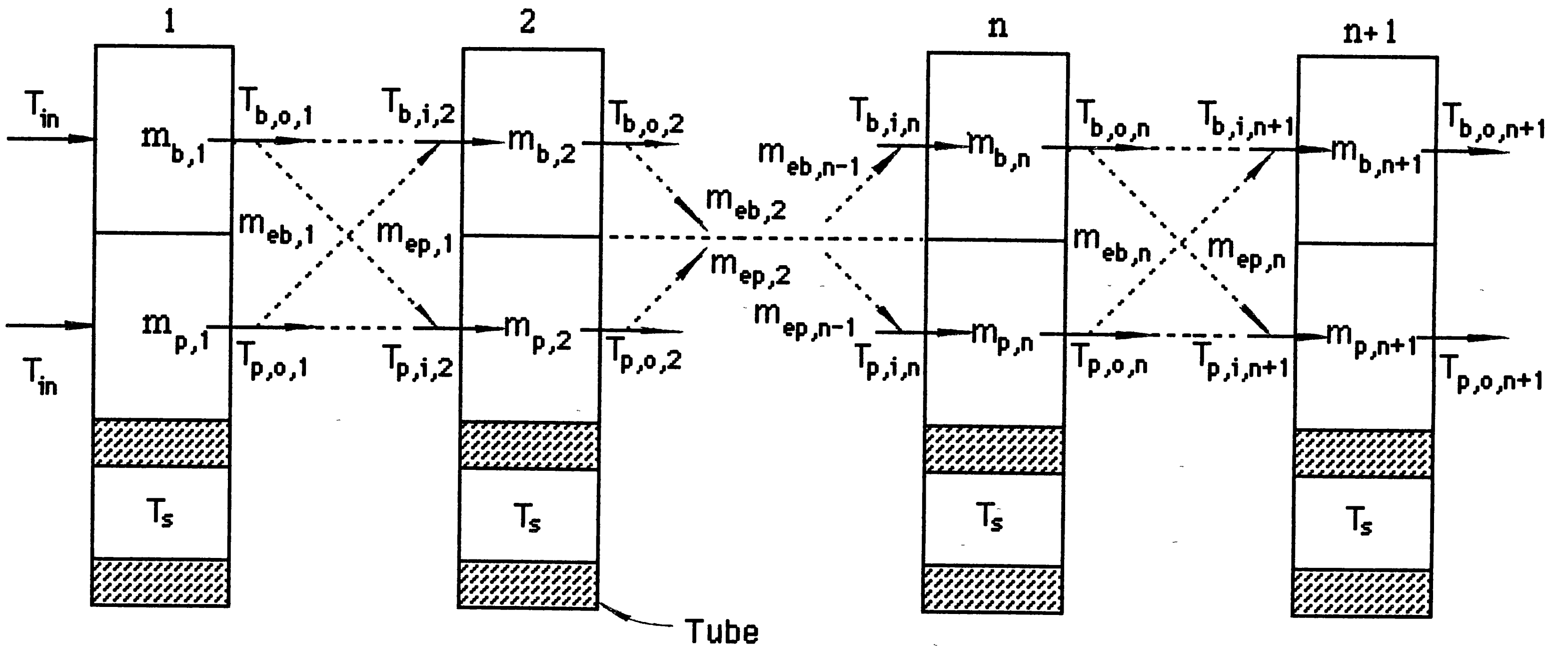

Figure 4. Diagram of the Postulated Streams in an Inline Bank with Finned Tubes

In this thesis, I develop a model which allows the primary, bypass, and interchange flows to vary from row to row. The new model is used to explain the row number effect problem.

CHAPTER II

LITERATURE REVIEW

There is much literature about the row number effect on heat transfer for inline finned tube banks, the thermal ineffectiveness of inline tube banks compared to staggered tube banks, and the bypass effect in inline tube banks. The row number effects for air cross flow outside tube banks were first studied by Pierson (1937) on plain tube banks. Weierman and Taborek (1978) and Rabas and Huber (1989) have investigated the row number effect in finned tube banks. Bell and Kegler (1978) presented a mathematical model of the effects of the interchange between the primary and bypass streams. The model in this paper is based on Bell and Kegler's model, but expanded and generalized to account for additional phenomena.

Row Number Effect in Plain Tube Banks

Pierson's (1937) measurements on a bank of plain tubes showed that not all the rows in the bank have the same heat transfer performance. He found that the first several rows in a plain tube bank have lower heat transfer coefficients than the rest of the tube rows.

Later, Kays and London (1954) found that the heat transfer coefficient increased with increasing number of tube rows, till it reached a constant value for deep tube banks (N_t greater than 10 tube rows). They found the row to row variation of the heat transfer coefficient (see Figure 5) for staggered tube banks, and they suggested that this relationship is suitable for inline tube banks also.

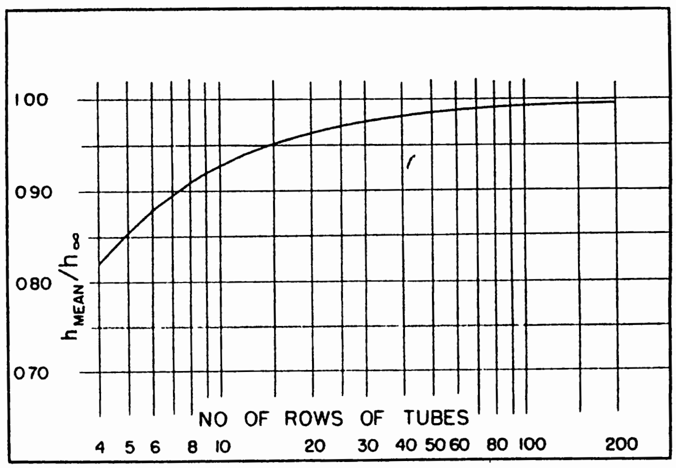

Figure 5. Influence of Row-to-Row Variation on Overall Unit Heat-Transfer Conductance From Kays and London (1954)

Zukauskas (1972) reached the same conclusion for Reynolds numbers greater than 1000. But, for Reynolds numbers between 100 and 1000, he found that the heat transfer coefficient is constant through the tube bank.

Zhang and Chen (1991) investigated inline tube banks with a longitudinal gap between the 3rd and 4th tube rows.

The ratios of pitches versus tube diameter are $p_t/d_r=3$ and $p_l/d_r=1.1$. The gap width (S_3) versus tube diameter varies from 1.1 (no gap) to 6. (The exact values of the tube diameter and pitches were not given.) The tube banks had 6 or 8 tube rows. The Reynolds number range is from 3,000 to 10,000. They concluded that the existence of a gap in the tube bank enhanced the heat transfer coefficient of those tubes adjacent to the gap by 10 to 30 percent. They found the row correction factors for tube banks with different gap widths (see Figure 6). Only the tube bank with 8 tube rows

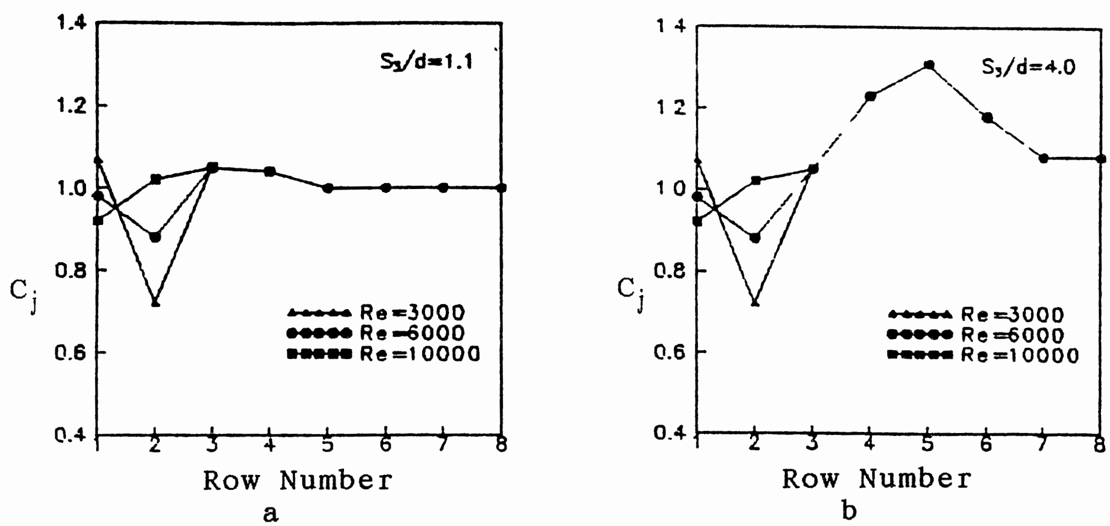

Figure 6. Row Correction Factor for Tube Banks with Different Gap Width From Zhang and Chen (1991)

is shown here. In the figure, C_j refers to the row correction factor $C_j=Nu_j/Nu_\infty$, where Nu_j is the Nusselt number of the nth tube row, and Nu_∞ is that of the deep tube bank. They found that the enhancement due to the gap reaches its maximum at $S_3/d=4.0$, and the heat transfer becomes fully developed at the eighth row ($C_8=1.0$). From Figure 4a (no gap tube bank), we find the following: At low Reynolds number (Re=3,000), the heat transfer coefficient decreases for the second tube row and then increases for the third row, remaining constant in the following tube rows. At high Reynolds numbers, the heat transfer coefficient increases until the third tube row and then stays constant for the remaining tube rows. Figure 6b shows the row correction factor for a tube bank with gap width of $S_3/d=4.0$. The existence of the gap enhanced the heat transfer rate in the downstream tube rows.

Row Number Effect on Finned Tube Bank

Carnavos (1958) did a group of experiments using Griscom-Russell K-Fin tubes. The tube and bank details are presented in Table 1 (next page). The ratios of the j factor for the inline tube bank to the j factor for the staggered tube bank are given below:

	d_r=0.377 in	d_r=0.188 in
Re=1,000	$j_{inline}/j_{staggered}=0.46$	$j_{inline}/j_{staggered}=0.47$
Re=6,000	$j_{inline}/j_{staggered}=0.60$	$j_{inline}/j_{staggered}=0.70$

From the above, we can see that the ratio is higher at the

TABLE 1

FINNED TUBE AND BANK GEOMETRY FOR EARLIER INVESTIGAT

Investigators	Test No.	Layout	Tube Bank Geometry			Finned Tube Geometry				
			N_t	P_t	P_l	d_r	d_f	n_f	t_f	w_s
Carnavos (1958)	1	Staggered	10	0.938	0.813	0.379	0.372	30	0.008	-
	2	"	"	1.188	"	"	"	"	"	-
	6	Inline	"	1.063	0.938	"	"	"	"	-
	7	"	"	0.938	"	"	"	"	"	-
	5	"	"	1.188	"	0.376	0.734	"	"	-
	10	Staggered	12	1.063	"	"	"	"	"	-
	3	"	10	1.188	0.813	0.378	0.749	24	0.009	-
	8	Inline	"	1.063	0.938	"	"	"	"	-
	4	"	"	1.188	0.813	0.377	0.739	16	0.008	-
	9	"	"	1.063	0.938	"	"	"	"	-
	11	"	"	0.531	0.469	"	"	30	"	-
	12	Staggered	"	0.594	0.406	"	"	"	"	-

TABLE 1 (Continued)

Investigators	Test No.	Layout	Tube Bank Geometry			Finned Tube Geometry				
			N_t	P_t	P_l	d_r	d_f	n_f	t_f	w_s
Ackerman & Brunsvold (1970)	1	Staggered	8	5.0	3.5	1.875	3.875	1.98	0.1	0.5
	2	"	"	6.0	3.25	"	"	"	0.125	"
	3	Inline	"	5.0	4.5	"	"	"	"	"
	4	"	"	"	"	"	"	"	"	"
	5	Staggered	"	5.0	3.25	"	"	"	"	"
	6	"	"	4.0	3.5	"	"	"	"	"
Weierman et al. (1978)	1	Inline	5	3.69	3.69	1.25	3.25	6.17	0.048	0.18
	2	"	2	"	"	"	"	"	"	"
	3	"	1	"	"	"	"	"	"	"
	4	"	7	4.50	4.50	2.0	4.03	5.94	"	0.17
	5	Staggered	5	"	3.90	"	"	"	"	"
Hashizume (1981)	-	Inline	"	1.81	1.81	0.75	1.65	7.47	0.016	0.118
	-	Staggered	"	"	1.65	"	"	"	"	"
Rabas & Eckels (1984)	1	Inline	3	3.75	3.75	1.25	3.25	6.02	0.048	0.156
	3	Staggered	"	"	3.25	"	"	6.35	"	"
	4	"	"	"	3.75	"	"	"	"	"

TABLE 1 (Continued)

Investigators	Test No.	Layout	Tube Bank Geometry			Finned Tube Geometry				
			N_t	P_t	P_l	d_r	d_f	n_f	t_f	w_s
Rabas & Eckels (1984) Cont.	6	Inline	3	3.75	3.75	1.25	3.25	6.02	0.048	0.156
	2	"	"	4.5	4.5	2.0	3.475	6.30	0.051	"
	5	"	"	6.0	"	"	4.0	"	0.048	"
	7	Staggered	"	"	"	"	"	"	"	"
Rabas & Huber (1989)	-	Inline	15	3.75	3.75	1.25	3.25	6.0	"	0.16
	-	Staggered	7	3.0	3.0	1.31	2.46	3.0	0.133	-

Note: All dimensions are inches.

higher Reynolds number. The finned tube bank with smaller root diameter has a higher ratio than the finned tube bank with larger root diameter.

Ackerman and Brunsvold (1970) did a set of experiments at Reynolds numbers ranging from 13,700 to 46,400 with 8 to 10 tube rows. See Table 1 for tube bank arrangements and geometries. With the same pitch ratio, the inline/staggered j factor ratio is 0.82 for the above Reynolds number range. For the staggered tube banks, their data shows that the heat transfer coefficient increases with increasing transverse tube pitch. The ratio remains the same for all the Reynolds numbers. This is not surprising, if the 8 tube rows deep bank has been noticed.

Hashizume (1981) gave a set of heat transfer data for both inline and staggered arrangements having 5 tube rows with the same fin geometries (height, thickness and pitch) but various fin configurations (spiral, plain, segment and semicircular). He concluded that there was no difference between the heat transfer performance of inline and staggered tube banks, contrary to other results. Rabas and Huber (1989) discussed this and pointed out that the different conclusion is due to Hashizume's experimental method. Hashizume measured the local heat transfer coefficients from a single thermally active tube in each of the rows. Rabas and Huber (1989) believe that this is not a valid method, especially for shallow tube banks. They said, "Because only one tube in the bank at a time is heated, this tube is not influenced by the temperature fields generated by the neighboring tubes" (page 26). However, they said that this method was suitable for staggered or deep inline tube banks.

Rabas and Huber (1989) presented a temperature profile of their experimental data. See Table 1 for tube bank arrangements and geometries. The temperature profile is shown in Figure 7 (Note: for the Re=21,000 run, the steam flow was cut off to the tubes of the first five rows, so heat transfer only began at the sixth row.) The temperature

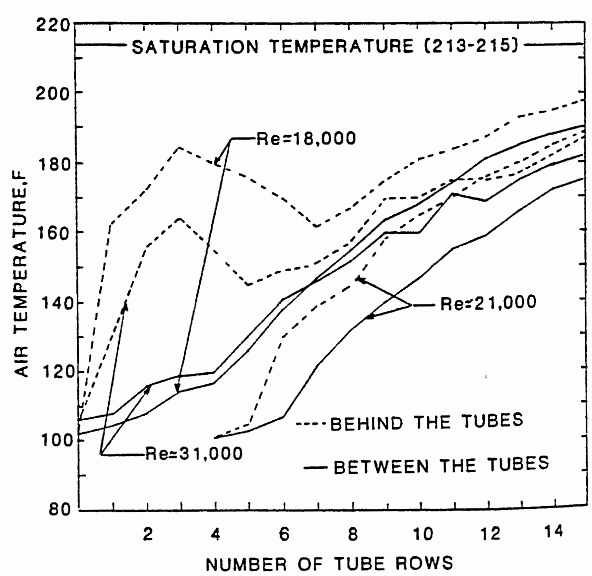

Figure 7. Temperatures Behind and Between the Tubes from Rabas and Huber (1989)

profiles are of two kinds: temperatures behind the tubes and temperatures between the tubes. From the Re=18,000 and Re=31,000 runs, we see that at the third tube row the temperature behind the tubes reaches a maximum and then decreases. After the 7th row for Re=18,000 run and 5th row for Re=31,000 run, the difference between the two temperatures becomes very small (within about 10 ^{0}F). The temperature profiles seem to do the following: There is an entrance effect, and several tube rows are required for the flow to become fully developed. The number of tube rows required for flow to be fully developed decreases with increasing Reynolds number.

Rabas and Eckels (1975) presented data comparing inline and staggered banks with only 3 rows of tubes and with various tube pitches. See Table 1 for tube bank arrangements and geometries. When the tube pitches are 3.75 inches (both transverse and longitudinal), the inline/staggered j factor ratio is about 0.50 at Re=4,000, and 0.70 at Re=20,000. When the tube pitches are 4.50 inches, the ratio is about 0.40 at Re=10,000, and is about 0.53 at Re=40,000.

Weierman et al. (1978) presented experimental results for inline tube banks with 1, 2, and 5 tube rows. Tube and bank details are presented in Table 1. Their data show that the heat transfer coefficient decreases with increasing number of tube rows. A comparison between inline and staggered tube banks is also given for a bank with 7 tube rows. The j factor of inline tube banks is only about 0.3 of the value for staggered tube banks.

Bypass Effect

Weierman et al. (1978) also presented a detailed study of temperature and velocity profiles between two transverse adjacent tubes. The tube and bank details are given in Table 1. The temperature and velocity profiles were presented for inline tube banks as well as staggered. For test No. 4, the temperature profiles are available behind the 2nd, 4th and 7th tube rows (see Figure 8a). (In Figure 8a, the solid lines represent the temperature after the

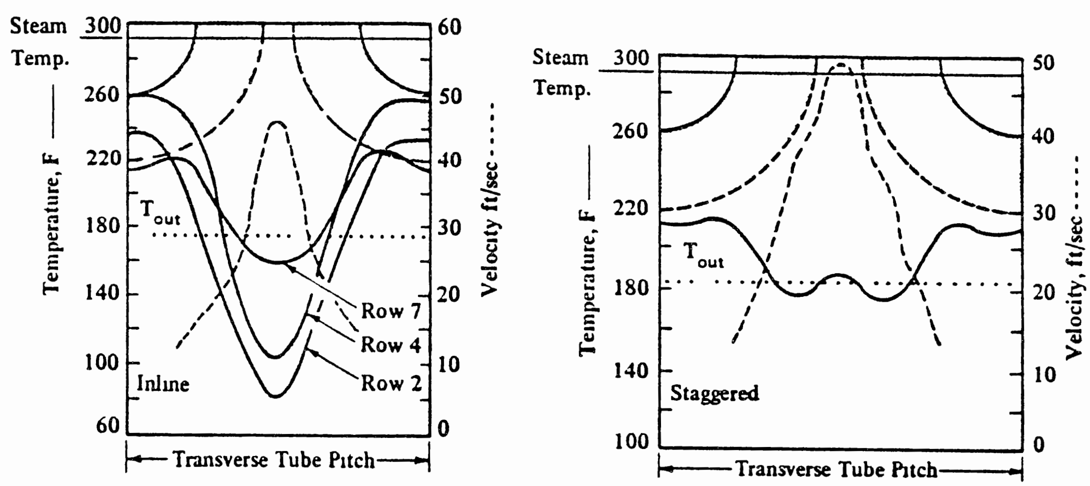

Test No. 4
a

Test No. 5
b

Figure 8. Temperature and Velocity Profiles between Two Transverse Adjacent Tubes from Weierman et al. (1978)

marked tube row, and the dashed lines represent the velocity profile after the 7th tube row.) From the figure, we seethat there is an obvious bypass flow existing between the tubes in inline tube banks. The bypass flow is much larger than the primary flow, and the temperature between the fin tips is much lower than that behind the tubes. On the other hand, the temperature is more uniform in staggered tube banks (see Figure 8b), though the velocity profile shows a steep change. (In Figure 8b, both the temperature and velocity profiles represent the temperature and velocity after the last tube row.) The temperature profile is consistent with Rabas's (1989) figure. Weierman's et al. results show that the temperature difference between the bypass and primary streams decreases with increasing number of tube rows. The primary stream temperature behind the 7th tube row is actually lower than that behind earlier tube rows. The stream that goes through the finned surface is heated quickly to a temperature much closer to the surface temperature than the mixed outlet temperature used in calculating the "apparent" Mean Temperature Difference. Weierman et al. concluded that the temperature profile is distorted, and therefore the simple LMTD formulation is incorrect. They also concluded that because less bypass exists in the staggered layout, it is more effective for heat transfer than the inline layout.

Also, Weierman et al. (1975) did an experiment for inline tube banks with sealing devices (a wood wedge and a plywood sheet) to block the bypass flow. See Figure 9 for details of the sealing devices. Since the bypass flow is reduced, a better heat transfer coefficient is obtained than in the inline tube bank, but with an increased pressure drop.

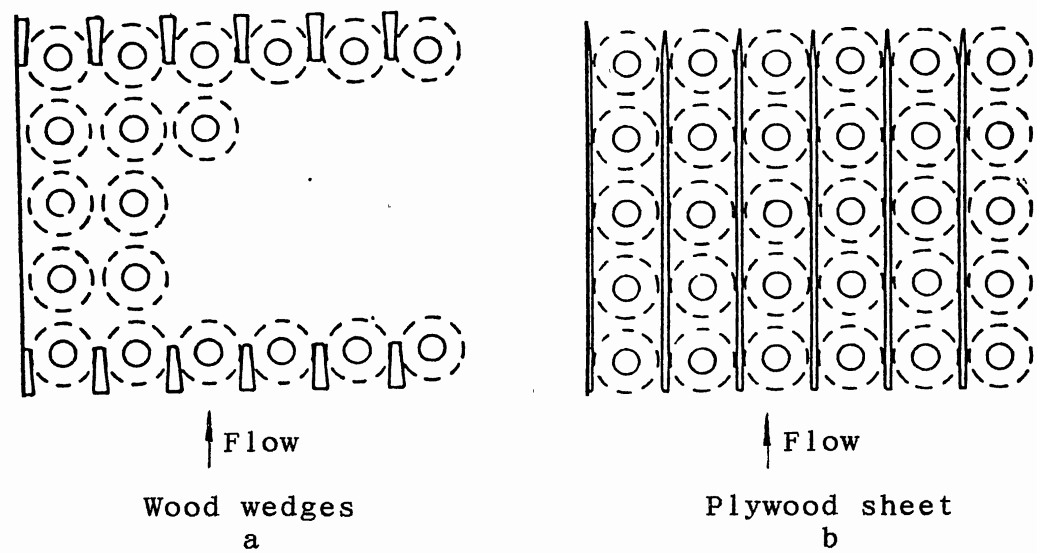

Figure 9. Sketch of Sealing Devices from Weierman et al. (1978)

Rabas and Eckels (1975) used several different kinds of sealing devices on a three row tube bank. By reducing the bypass flow, the heat transfer coefficient of the tube bank with enhancements (sealing devices) is better than that of the inline tube banks. But, it is still lower than that of the staggered tube banks. So, Rabas and Eckels recommended the staggered tube bank.

Bell and Kegler (1978) presented a mathematical analysis of the effect of bypassing in an exchanger having an isothermal tube surface. They abandoned the traditional LMTD method and used a two stream approach. They divided the air flow into two parts: the bypass flow and the primary flow. The bypass flow exists between the outer portion of the fins, contacts little heat transfer surface and has a higher velocity. The primary flow exists between the fins and has a lower flow velocity. Between the bypass and primary streams, there is an interchange flow. The model is described in Figure 3.

From the heat balance, they found the differential equations for the rate of temperature change of each of the two streams:

Bypass stream $\quad dT_b/dx = (w/W_b)(T_p-T_b) \qquad (7)$

Primary stream $\quad dT_p/dx = (w/W_p)(T_b-T_p)-U_0a(T_p-T_s)/W_pc_p \qquad (8)$

Solving the differential equations gives the two equations:

$$\frac{T_b-T_s}{T_o-T_s} = -\frac{q}{p-q}e^{px} + \frac{p}{p-q}e^{qx} \qquad (9)$$

and

$$\frac{T_p-T_s}{T_o-T_s} = -\frac{q}{p-q}(1+\frac{p}{\alpha})e^{px}+\frac{p}{p-q}+\frac{p}{\alpha}\frac{p}{p-q}e^{qx} \qquad (10)$$

where

$$p = \frac{1}{2}(-(\alpha+\beta+\gamma)+\sqrt{(\alpha+\beta+\gamma)^2-4\alpha\gamma}) \tag{11}$$

$$q = \frac{1}{2}(-(\alpha+\beta+\gamma)-\sqrt{(\alpha+\beta+\gamma)^2-4\alpha\gamma}) \tag{12}$$

and

$$\alpha = w/W_b; \quad \beta = w/W_p; \quad \gamma = U_o a/W_p c_p. \tag{13}$$

Bell and Kegler used the experimental data of Weierman et al. (1978), which were taken at conditions close to the assumptions in the model. For the inline tube bank, they found a real heat transfer coefficient, U_0, which was close to the value predicted for the staggered array. They concluded that the generally accepted correlation for finned tube heat transfer coefficient in staggered tube banks was applicable to inline tube banks as well where the bypass stream effects on velocity and temperature profile are taken into account.

CHAPTER III

DERIVATION OF MATHEMATICAL MODEL

In this model, a two stream approach is used. As soon as the gas flow comes into the tube bank, the stream divides to two parallel streams. One is the bypass flow. It flows between the tubes (mainly between the fin tips of adjacent tubes, although the outer region of the fins is also involved), and has a flow rate of m_b (lbm/hr). It is assumed to contact no heat transfer surface. The other stream is the primary flow, which flows between the fins. The primary flow has a flow rate of m_p (lbm/hr). It contacts the heat transfer surface. It is assumed that, when the gas flows through a tube row, the two streams do not interact with each other (as shown by Figure 4). However, when the gas flows from one tube row to the other, the two streams interchange mass with each other. There is an interchange flow at a rate m_{ep} from the primary flow to the bypass flow, and another interchange flow at a rate m_{eb} from the bypass flow to primary flow. The interchange streams provide the only mechanism by which the temperature of the bypass stream can change. Figure 4 (page 7) describes the basic idea of this model. It is used as the basis for deriving the mathematical model. The figure is also helpful for the reader to become familiar with the symbols used in the model. In the model, the subscript 'b' refers to the bypass stream, 'p' refers to the primary stream, 'eb' refers to the interchange stream that from bypass stream to primary stream, 'ep' refers to the interchange stream that from primary stream to bypass stream, 'i' refers to the stream entering a tube row, and 'o' refers the stream exiting a tube row, the last subscript refers to the tube row number.

The Basic Derivation

When developing the model, the following assumptions were made:

1. Heat capacity of the gas is a constant throughout the tube bank.
2. The bypass and primary heat transfer streams are flowing perpendicular to the axes of the tubes.
3. Interchange streams only occur between the tube rows.
4. Convective heat transfer between the bypass and the primary streams is negligible
5. The heat transfer coefficient between the tube and the primary stream is a constant for a given tube row.
6. Between two given tube rows (row n and row n+1), the interchange flow rates $m_{ep,n}$ and $m_{eb,n}$ are constants.
7. Tube side fluid is isothermal.
8. The mixing process between the interchange streams and the primary and bypass streams is adiabatic.

The mass balance and the heat balance were constructed separately for flows through the tube row and for flows between tube rows.

Governing Equations

1. For streams flowing through the nth tube row:

Since there is no interchange flow here, no mass balance is needed.

Heat balance

$$T_{b,i,n} = T_{b,o,n} \tag{14}$$

$$m_{p,n} * c_p * (T_{p,o,n} - T_{p,i,n}) = U_{p,n} * A_{tot}\, MTD \tag{15}$$

where:

$$MTD = \begin{cases} LMTD = \dfrac{T_{p,o,n} - T_{p,i,n}}{\ln\dfrac{(T_s - T_{p,i,n})}{(T_s - T_{p,o,n})}} & (16) \\ \text{or} & \\ AMTD = T_s - \dfrac{T_{p,i,n} - T_{p,o,n}}{2} & (17) \end{cases}$$

where:

$T_{b,i,n}$= Bypass stream temperature entering the nth tube row; ^{0}F or K

$T_{b,o,n}$= Bypass stream temperature exiting the nth tube row; ^{0}F or K

$T_{p,i,n}$= Primary stream temperature entering the nth tube row; ^{0}F or K

$T_{p,o,n}$ = Primary stream temperature exiting the nth tube row; ^0F or K

T_s = Tube side stream temperature; ^0F or K

$m_{p,n}$ = Primary stream flow rate at nth tube row; lbm/hr or kg/s

$U_{p,n}$ = Overall heat transfer coefficient for primary flow at nth tube row (based on total outside surface area); Btu/(hr-ft^2-^{0}F) or W/(m^2-K)

2. For streams flowing between the nth and (n+1)th tube rows

Mass balance

$$m_{b,n+1} = m_{b,n} + m_{ep,n} - m_{eb,n} \tag{18}$$

$$m_{p,n+1} = m_{p,n} + m_{eb,n} - m_{ep,n} \tag{19}$$

where:

$m_{b,n}$ = Bypass flow rate at nth tube row; lbm/hr or kg/s

$m_{b,n+1}$ = Bypass flow rate at (n+1)th tube row; lbm/hr or kg/s

$m_{p,n+1}$ = Primary flow rate at (n+1)th tube row; lbm/hr or kg/s

$m_{eb,n}$ = Interchange flow rate for stream from bypass to primary between nth and (n+1)th tube row; lbm/hr or kg/s

$m_{ep,n}$ = Interchange flow rate for stream from primary to bypass between nth and (n+1)th tube row; lbm/hr or kg/s

Heat balance

$$m_{b,n}C_pT_{b,o,n} + m_{p,n}C_pT_{p,o,n} = m_{b,n+1}C_pT_{b,i,n+1} + m_{p,n+1}C_pT_{p,i,n+1} \quad (20)$$

$$m_{b,n}C_pT_{b,o,n} - m_{eb,n}C_pT_{b,o,n} + m_{ep,n}C_pT_{p,o,n} = m_{b,n+1}C_pT_{b,i,n+1} \quad (21)$$

$$m_{p,n}C_pT_{p,o,n} - m_{ep,n}C_pT_{p,o,n} + m_{eb,n}C_pT_{b,o,n} = m_{p,n+1}C_pT_{p,i,n+1} \quad (22)$$

where:

$T_{b,i,n+1}$= Bypass stream temperature for stream into (n+1)th tube row; ^{0}F or K

$T_{p,o,n+1}$= Primary stream temperature for stream out of (n+1)th tube row; ^{0}F or K

Since the heat capacity is assumed to be constant throughout the tube bank, the above heat balance equations become

$$m_{b,n}T_{b,o,n} + m_{p,n}T_{p,o,n} = m_{b,n+1}T_{b,i,n+1} + m_{p,n+1}T_{p,i,n+1} \quad (23)$$

$$m_{b,n}T_{b,o,n} - m_{eb,n}T_{b,o,n} + m_{ep,n}T_{p,o,n} = m_{b,n+1}T_{b,i,n+1} \quad (24)$$

$$m_{p,n}T_{p,o,n} - m_{ep,n}T_{p,o,n} + m_{eb,n}T_{b,o,n} = m_{p,n+1}T_{p,i,n+1} \quad (25)$$

The above model is developed to suit the general case. Since we do not know how the bypass and primary heat transfer streams change from row to row, we assumed the two interchange flow rates are equal between two given tube rows. Then, the bypass flow rate and primary flow rate become constants throughout the tube bank. Below is the equation simplified for this case.

For stream flow through nth tube row:

Heat balance

$$T_{b,i,n} = T_{b,o,n} \tag{26}$$

$$m_{p,n}C_p(T_{p,o,n} - T_{p,i,n}) = U_{p,n}A_{tot}MTD \tag{27}$$

For stream flow between the nth and (n+1)th rows:

Mass balance

$$m_{eb,n} = m_{ep,n} = m_{e,n} \tag{28}$$

$$m_{b,n} = m_{b,n+1} = m_b \tag{29}$$

$$m_{p,n} = m_{p,n+1} = m_p \tag{30}$$

Heat balance

$$m_bC_pT_{b,o,n} + m_pC_pT_{p,o,n} = m_bC_pT_{b,i,n+1} + m_pC_pT_{p,i,n+1} \tag{31}$$

$$m_bC_pT_{b,o,n} - m_{e,n}C_pT_{b,o,n} + m_{e,n}C_pT_{p,o,n} = m_bC_pT_{b,i,n+1} \tag{32}$$

$$m_pC_pT_{p,o,n} - m_{e,n}C_pT_{p,o,n} + m_{e,n}C_pT_{b,o,n} = m_pC_pT_{p,i,n+1} \tag{33}$$

Since the heat capacity is assumed to be constant throughout the tube bank, the above heat balance equations become

$$m_bT_{b,o,n} + m_pT_{p,o,n} = m_bT_{b,i,n+1} + m_pT_{p,i,n+1} \tag{34}$$

$$m_bT_{b,o,n} - m_{e,n}T_{b,o,n} + m_{e,n}T_{p,o,n} = m_bT_{b,i,n+1} \tag{35}$$

$$m_pT_{p,o,n} - m_{e,n}T_{p,o,n} + m_{e,n}T_{b,o,n} = m_pT_{p,i,n+1} \tag{36}$$

CHAPTER IV

INTERPRETATION OF THE DATA IN LIGHT OF THE MODEL

The model is developed and tested by using the temperature profile data (see Figure 7) of Rabas and Huber (1989). The data from this profile has been read out and is listed in Table 2. The arrangement of their experiment is close to the two stream assumption of the model. The temperatures behind the tubes and between the tubes in their experiment are very close to the primary and bypass temperatures defined in this model.

Description of the Experiment

In Figure 7, the temperatures between and behind the tubes are plotted as a function of the number of tube rows for a 15-row tube bank for three different runs. The three runs are: the Re=18,000 and the Re=31,000 run with all the tubes thermally active, and the Re=21,000 run with only the last 10 rows of tubes thermally active. The heat source is steam condensing inside vertical tubes at a pressure slightly greater than atmospheric. The saturation temperature of the condensing steam is about 215 ^{0}F. The steam flow was cut off to the tubes of the first five rows

TABLE 2

EXPERIMENTAL DATA OF TEMPERATURES BEHIND AND BETWEEN THE TUBE ROWS BY RABAS AND HUBER (1989)

Row No.	Re=18,000		Re=21,000		Re=31,000	
	T_b ^0F	T_p ^0F	T_b ^0F	T_p ^0F	T_b ^0F	T_p ^0F
0	102	102			106	106
1	104	163			108	
2	108	172			117	155
3	114	184			119	163
4	116	180	100	100	120	155
5	124	175	102	105	130	143
6	137	169	107	130	141	148
7	146	162	121	139	146	150
8	154	167	132	144	151	155
9	162	174	141	158	159	169
10	167	181	148	164	158	169
11	173	183	155	170	171	174
12	182	188	159	175	168	174
13	185	192	165	180	173	176
14	188	195	172	184	178	182
15	190	197	174	190	182	188

Note: In this table, 'T_b' refers to the temperatures between the tubes, and 'T_p' refers to the temperatures behind the tubes.

for the third run. The test unit is 15 rows deep and contained four tubes per row. The tube bank arrangement was inline. The forced draft arrangement was used. An entrance section exists to dampen the non-uniformity of the approach air velocity profile. The tube length was 305mm (1 ft). The tube and bank details are listed in Table 1. The condensate from each tube row was collected and measured. The temperatures were measured by a digital temperature recorder. The same device was used for all the readings. The same probe holes were always used, and the probes were always extended the same depth into the tube bank.

With the geometries in Table 1, we can compute some more geometry information that we need. The equations are from Weierman and Taborek (1978).

1. Total outside surface area per unit length; A_0

$$A_o = \pi d_r(1 - t_f n_f) + 2n_f\left(\frac{\pi}{4}\right)[(d_f - 2l_c)^2 - d_r^2] \qquad (37)$$

$$+ N_t[2l_c(t_f + w_s) + t_f + w_s]$$

where

l_c is assumed to be 0.067ft which is $0.8l_f$. (In the original paper, Rabas and Huber (1989) did not give this geometry. I have assumed this number according to other similar fin tubes.)

Hence

$$A_0 = \pi*0.104*(1-0.104*6)+2*6*(\pi/4)*[(0.271-2*0.067)^2-0.104^2]+31*[2*0.067*(0.004+0.013)+0.004*0.013]$$

$$= 6.36\ ft^2/ft$$

2. Total outside effective heat transfer surface area per row; A_{tot}

$$A_{tot} = A_o L (N_t)_t + A_{ts} \tag{38}$$

where

$$(N_t)_t = (N_t)_{row} = 4$$

and $A_{ts} = 0$ (Assumed).

Hence:

$$A_{tot} = 6.36 * 1.0 * 4 = 25.4 \quad ft^2/row$$

for the whole tube bank:

$$(A_{tot})_{15\ rows} = 25.5 * 15 = 382.5 \quad ft.$$

3. Minimum flow area; A_{min}

$$A_{min} = (N_t)_{row} L (p_t - d_r - 2 n_f l_f t_f) + x, \tag{39}$$

where x = 0 (assumed).

Hence:

$$A_{min} = 4*1*(0.312-0.104-2*(6*12)*0.083*0.004$$
$$= 0.642 \ ft^2.$$

4. Fin outside area per unit length; $(A_f)_0$

$$(A_f)_o = A_o - \pi d_r (1 - t_f n_f). \tag{40}$$

Hence:

$$(A_f)_0 = 6.36-\pi*0.104*(1-0.004*(6.0*12))$$
$$= 6.13 \ ft^2/ft.$$

5. Tube inside area per unit length; A_i

$$A_i = \pi d_i, \tag{41}$$

where

$$d_i = 1.05 \text{ in.}$$

Hence:

$$A_i = \pi*1.05/12 = 0.275 \text{ ft}^2/\text{ft}.$$

Estimation of Air Flow Rate

The total flow rate of air was not given by Rabas and Huber (1989). The only information given that related to the flow rate is the Reynolds number. I backed out the total air flow rate from the Reynolds number,

$$Re = G_{max} d_r / \mu \tag{1}$$

where μ was selected as $13.6*10^{-6}$ lbm/(ft-sec) at an air temperature of 150 ^{0}F.

Hence:

$$\begin{aligned} G_{max} &= Re*\mu/d_r \\ &= 1800*13.6*10^{-6}/0.104 \\ &= 2.35 \text{ lbm/(ft}^2\text{-s)}, \end{aligned}$$

and

$$\begin{aligned} M &= G_{max} A_{min} \\ &= 2.35*0.642 \\ &= 1.5 \text{ lbm/s} = 5400 \text{ lbm/hr}. \end{aligned}$$

Now, we have the total flow rate of air. But, this still can not be applied in the model. We must know the bypass and primary stream mass flow rates. Weierman et al. (1978) did a detailed study of temperature and velocity distributions behind the tube row (see Figure 8). From the velocity profile, we can calculate the bypass and primary flow rates. Bell and Kegler (1978) used two of Weierman's profiles to test their model. They integrated the velocity profiles numerically to get the bypass and primary flow rates. I followed their steps to calculate the bypass and primary flow rates with the rest of the profiles. The calculation results of both Bell and Kegler's as well as my own results are listed in Table 3. From the table, we find

TABLE 3

BYPASS AND PRIMARY FLOW RATES CALCULATED FROM THE VELOCITY PROFILES OF WEIERMAN ET AL. (1978)

Layout	Row Number	M (lbm/hr)	m_b (lbm/hr)	m_p (lbm/hr)
Inline	2	107,520	73,144	34,376
Inline	2	22,260	15,506	6,753
Inline	1	107,340	58,608	48,732
Inline	1	22,260	15,092	7,168
Inline	7	108,180	65,241	42,939
Inline	7	21,900	18,140	3,760

the following: After the first row, the primary flow rate is about 45 percent of the total flow rate; after the 2nd and

7th rows, the primary flow rate is about 20 to 30 percent of the total flow rate. Thus, it is possible for the first row to have a larger primary flow fraction than that of the rest of the tube rows. This difference may due to the different stream flow pattern between the first row and the rest of the tube rows (see Figure 10).

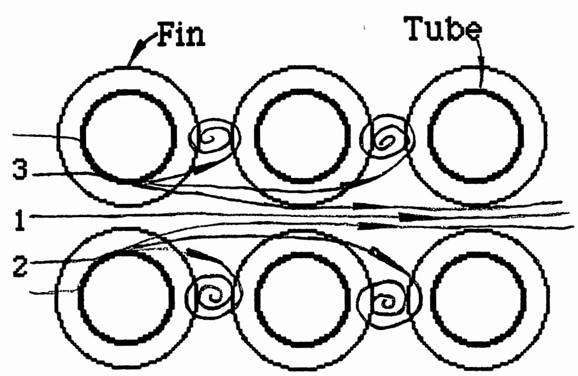

Figure 10. Possible Stream Flow Pattern in Inline Finned Tube Bank

From Figure 10, we see that stream line 1 is always a bypass stream throughout the whole tube bank. But, stream lines 2 and 3 belong to the primary flow for the first tube row, and then they become part of the bypass flow throughout the rest of the tube bank. The fin tube geometries and tube bank arrangement of Weierman et al.'s experiment are close to those of Rabas and Huber. So, I assumed that the proportion of the primary flow rate to the total flow rate in Rabas and Huber's experiment is close to that of Weierman et al.'s. The assumed bypass and primary flow rate are listed in Table 4. (In the table, only data for the Re=18,000 and the Re=31,000 runs are listed. For the Re=21,000 run, since only the last 10 tube rows are thermally effective, a uniform m_b = 4480 lbm/hr and m_p = 1920 lbm/hr was assumed.)

The Re = 18,000 run was selected for the sample calculation. I assume $m_p = (1/3)M$ through out the tube bank.

Hence:

$$m_p = (1/3)*5400 = 1800 \text{ lbm/hr},$$

and

$$m_b = M-m_p = 5400-1800 = 3600 \text{ lbm/hr}.$$

Thermal Calculations

Rabas and Huber's experimental data are not detailed enough to calculate the air side heat transfer coefficients and the interchange flow rates. Rabas and Huber (1989) said, "however, the row-by-row heat transfer data were not considered to be of the quality required for publication" (page 28). What I did here was to assume the air side heat transfer coefficients of the primary flow and the interchange flow rates, put these into the model, and check whether the results fit the experimental data or not.

TABLE 4

BYPASS AND PRIMARY FLOW RATE ASSUMED IN THE MODEL

Row Number	Re=18,000				Re=31,000			
	Case 1		Case 2		Case 1		Case 2	
	m_p	m_b	m_p	m_b	m_p	m_b	m_p	m_b
1	1800	3600	2160	3240	3100	6260	3744	5616
2	1800	3600	1782	3618	3100	6260	3089	6271

Note: All the units are lbm/hr. In the table, 'Case 1' assumes a uniform bypass and primary flow rates were assumed, and 'Case 2' assumes non-uniform bypass and primary flow rates. After the second tube row, the bypass and primary flow rates are assumed to remain the same in both cases.

Kays and London (1954) found that even the staggered tube banks (which presumably have little bypass flow) also had a row number effect. They found that the heat transfer coefficients increased with increasing number of tube rows for staggered tube banks. So, besides the bypass flow, other factors affecting heat transfer may vary from row to row. In this thesis, the heat transfer coefficients for primary flow are assumed to increase during stream flow through the first several tube rows, and then reach a constant value throughout the rest of the tube bank.

The interchange flow rates are also assumed to increase through the first several tube rows, and then reach a constant value throughout the rest of the tube bank. I made this assumption because the tubes themselves and the fins on the tubes are turbulence promoters. So, the turbulence level increases through the first several tube rows, and the flow becomes fully developed for the rest of the tube rows. The interchange flow rates change along with the turbulence level.

The assumed heat transfer coefficient may be the film heat transfer coefficient with 100 percent fin efficiency for primary flow (h_{cp}), the actual film heat transfer coefficient for primary flow (h_{ap}), or the overall heat transfer coefficient for primary stream (U_p). If the h_{ap} or the U_p is assumed, finding the film heat transfer coefficient requires trial and error. The evaluation of equations in Chapter III can be done by hand. Since many different tries are required to test the model, a computer program was developed to reduce the calculation work. The estimations of the interchange flow rates and heat transfer coefficients for primary flow were read from an input data file. The programmer must first edit the data file, then runs the program. From the output of the program, the programmer judges the results and modifies the estimates, until the calculated value was close to that of the experimental data. Either the U_p and h_{cp} can be the input of the program. The computer program is given in Appendix C.

The Re=18,000 run was selected for the sample calculation. The assumed heat transfer coefficients with 100 percent fin efficiency for primary flow (h_{cp}) and the interchange flow rates are listed in Table 5. Since the calculation procedures for all tube rows are the same, the sample calculation is only given for the first and second rows.

The overall heat transfer coefficients are computed first. The procedures are:

1. Thermal resistance R_{th} (It accounts for both the stream side convective resistance and the tube wall conductive resistance. Also, it is based on the total outside surface area.)

$$R_{th}=A_o\frac{\ln(d_o/d_i)}{2\pi k}+\frac{(A_o/A_i)}{h_i}, \tag{42}$$

TABLE 5

ASSUMED HEAT TRANSFER COEFFICIENTS
AND INTERCHANGE FLOW RATES

Row No.	Re=18,000		Re=21,000		Re=31,000	
	h_{cp}	m_e/M	h_{cp}	m_e/M	h_{cp}	m_e/M
1	11.0	0.02			15.3	0.03
2	12.0	0.04			16.7	0.05
3	13.0	0.06			18.1	0.07
4	14.0	0.08			18.8	0.09
5	14.5	0.10			19.5	0.11
6	15.0	0.11	15.6	0.11	20.2	0.12
7	15.0	0.12	16.5	0.12	20.9	0.13
8	15.0	0.135	16.5	0.135	20.9	0.135
9	15.0	0.135	16.5	0.135	20.9	0.135
10	15.0	0.135	16.5	0.135	20.9	0.135
11	15.0	0.135	16.5	0.135	20.9	0.135
12	15.0	0.135	16.5	0.135	20.9	0.135
13	15.0	0.135	16.5	0.135	20.9	0.135
14	15.0	0.135	16.5	0.135	20.9	0.135
15	15.0	0.135	16.5	0.135	20.9	0.135

Note: The unit of h_{cp} is Btu/(hr-ft^2-^{0}F). The above estimated m_e/M is assumed with a uniform primary flow rate. For the nun-uniform primary flow rate case, I assume $m_{eb,1}/M = 0.02$, $m_{ep,1}/M = 0.09$ for Re=18,000 Run, and $m_{eb,1}/M = 0.03$, $m_{ep,1}/M = 0.10$ for Re=31,000 Run. All other $m_{eb,n}/M$ and $m_{ep,n}/M$ are assumed the same as that listed in the table.

where

$k = 30.3$ Btu/(hr-ft-^{0}F) (From Rabas and Eckel (1975) with similar tube geometries)

and

$h_i = 2{,}000$ Btu/(hr-ft^2-^{0}F) (based on inside tube area).

Hence:

$$R_{th} = 6.36\frac{\ln(0.104/0.0875)}{2*\pi*30.3} + \frac{(6.36/0.275)}{2000}$$

$=0.0174$ (hr-ft^2-^{0}F)/Btu.

2. Overall heat transfer coefficient $U_{p,n}$ (based on total outside surface area);

a. Actual film heat transfer coefficient $h_{ap,n}$ (based on total outside effective heat transfer area)

$$h_{cp,n} = \frac{h_{ap,j}}{1-(1-\Omega)(A_f)_o/A_o} \tag{44}$$

where

$$\Omega = \frac{\tanh(zl_e)}{(zl_e)} \tag{5}$$

and

$$l_e = l_f; \quad z = \sqrt{\frac{2h_c}{k_f t_f}}; \text{ and } t_e = \frac{t_f w_s}{t_f + w_s}. \tag{6}$$

From

$t_f = 0.0040$ ft ; $w_s = 0.0132$ ft,

we get

$$t_e = \frac{0.004*0.0132}{0.004+0.0132} = 0.0031ft.$$

Hence, for the first tube row:

$$z = (\frac{2*11.0}{30.3*0.0031})^{1/2} = 15.3 \quad ft^{-1},$$

$$\Omega = \frac{\tanh(15.3*0.0833)}{(15.3*0.0833)} = 0.671$$

$$h_{ap,1} = h_{cp,1}[1-(1-\Omega)(A_f)_o/A_o]$$

$$= 11.0*[1-(1-0.671)*6.13/6.36]$$

$$= 7.51 \; Btu/(hr\text{-}ft^2\text{-}{}^oF),$$

and for the second tube row:

$$\Omega = \frac{\tanh(16.0*0.0833)}{16.0*0.0833} = 0.653$$

$$h_{ap,2} = 12.0*[1-(1-0.653)*6.13/6.36]$$

$$= 7.99 \; Btu/(hr\text{-}ft^2\text{-}{}^oF).$$

b. Overall heat transfer coefficient $U_{p,n}$ (based on the total outside surface area):

$$U_{p,n} = \frac{1}{\frac{1}{h_{ap,n}} + R_{th}}. \tag{45}$$

For the first tube row

$$U_{p,1} = \frac{1}{\frac{1}{7.51}+0.0174} = 6.64 \quad Btu/(hr\text{-}ft^2\text{-}{}^oF).$$

For the second tube row

$$U_{p,2} = \frac{1}{\frac{1}{7.99}+0.0174} = 7.01 \ \ Btu/(hr\text{-}ft^2\text{-}^oF).$$

Now, we can use the model to calculate the row by row bypass and primary temperatures. The air comes in at a uniform temperature of 102 ^{0}F.

For the first row:

Heat balance:

$$T_{b,o,1} = T_{b,i,1} = 102^oF$$

$$m_p c_p (T_{p,o,1} - T_{p,i,1}) = U_{p,1} A_{tot} \frac{T_{p,o,1} - T_{p,i,1}}{\ln(\frac{T_s - T_{p,i,1}}{T_s - T_{p,o,1}})},$$

we have

$$\frac{T_s - T_{p,i,1}}{T_s - T_{p,o,1}} = Exp(\frac{U_{p,1} A_{tot}}{m_p c_p}),$$

where

T_s = 215 ^{0}F

m_p = 1800 lbm/hr

and c_p = 0.24 Btu/(lbm-^{0}F).

Hence:

$$\frac{215-102}{215-T_{p,o,1}} = Exp(\frac{6.63*25.5}{1800*0.24})$$

$T_{p,o,1}$ =138.9 ^{0}F.

For the gap between first and second row:

Heat balance

$$m_b(T_{b,i,2} - T_{b,o,1}) = m_p(T_{p,o,1} - T_{p,i,2}) = m_{e,1}(T_{p,o,1} - T_{b,o,1}).$$

Assume:

$$m_{e,1} = 0.02M,$$

where

M = 5400 lbm/hr (total stream mass flow rate).

Hence:

$$3600*(T_{b,i,2}-102) = 1800*(138.9-T_{p,i,2}) = 0.02*5400*(138.9-102)$$

$$T_{b,2,i} = 103.1\ ^0F \quad ; \quad T_{p,i,2} = 136.7\ ^0F.$$

For the second row:

Heat balance

$$T_{b,o,2} = T_{b,i,2}$$

$$\frac{T_s - T_{p,i,2}}{T_s - T_{p,o,2}} = Exp(\frac{U_{p,2}A_{tot}}{m_pC_p}).$$

Hence:

$$T_{b,o,2} = 103.1\ ^0F$$

$$\frac{215-136.7}{215-T_{p,o,2}} = Exp(\frac{7.01*25.5}{1800*0.24})$$

$$T_{p,o,2} = 163.2\ ^0F.$$

For the gap between second and third row:

Heat balance:

$$m_b(T_{b,i,3} - T_{b,o,2}) = m_p(T_{p,o,3} - T_{p,i,3}) = m_{e,2}(T_{p,o,2} - T_{b,o,2}).$$

Assume:

$$m_{e,2} = 0.04M$$

hence

$$3600 * (T_{b,i,3} - 103.1) = 1800 * (163.2 - T_{p,i,3})$$

$$= 0.04 * 5400 * (163.2 - 103.1)$$

$$T_{b,i,3} = 106.7\ {}^{0}\mathrm{F} \quad ; \quad T_{p,i,3} = 156.0\ {}^{0}\mathrm{F}$$

(The above values are close to those from the computer output that listed in Table 6.)

TABLE 6

BYPASS AND PRIMARY TEMPERATURES CALCULATED FROM THE MODEL OF Re=18,000 RUN

Row No.	Uniform m_b and m_p				Non-uniform m_b and m_p			
	$T_{b,i}$ ^0F	$T_{p,i}$ ^0F	$T_{b,o}$ ^0F	$T_{p,o}$ ^0F	$T_{b,i}$ ^0F	$T_{p,i}$ ^0F	$T_{b,o}$ ^0F	$T_{p,o}$ ^0F
0	102.0	102.0	102.0	138.6	102.0	102.0	102.0	133.4
1	103.1	136.4	103.1	163.0	106.2	131.5	106.2	160.0
2	106.7	155.8	106.7	176.6	109.4	153.5	109.4	175.3
3	113.0	164.0	113.0	182.3	115.3	163.3	115.3	182.0
4	121.3	165.7	121.3	183.6	123.3	165.8	123.3	183.9
5	130.7	164.9	130.7	183.5	132.3	165.5	132.3	184.0
6	139.4	166.0	139.4	184.5	140.8	166.8	140.8	185.1
7	147.5	168.2	147.5	185.8	148.7	169.0	148.7	186.4
8	155.2	170.3	155.2	187.1	156.3	171.0	156.3	187.7
9	161.7	174.2	161.7	189.5	162.6	174.9	162.6	190.1
10	167.3	178.3	167.3	192.1	168.2	178.9	168.2	192.6
11	172.3	182.1	172.3	194.4	173.1	182.6	173.1	194.9
12	176.8	185.5	176.8	196.6	177.5	186.0	177.5	197.0
13	180.8	188.6	180.8	198.5	181.4	189.0	181.4	198.9
14	184.4	191.4	184.4	200.2	184.9	191.7	184.9	200.5
15	187.6	193.8	187.6	193.8	188.1	194.1	188.1	194.1

Note: All the units are ^0F.

CHAPTER V

DISCUSSION OF THE MODEL

The results of several trials using the model are listed in Tables 6, 7, and 8. The bypass and primary temperatures, and the difference between them, are plotted as functions of tube row number in Figure 11-25. (Figure 17-25 are in Appendix A.) The computational results are drawn on the same figure with the experimental results. From these Figures, we see that the model fits the experimental data generally. And, checking the estimations of the heat transfer coefficients and the interchange flow rates, they are also within reasonable ranges.

From the Figures, we see that the calculated values from the model show the same temperature distributions as that of the experimental data. From both the calculated data and the experimental data, we can divide the tube bank into three regions: entrance, transition, and fully developed region. In the entrance region, the primary flow temperature increases quickly as soon as the flow enters the heat exchanger; at the same time, the bypass flow temperature increases only a little, but the temperature difference between the two streams also increases quickly.

TABLE 7

BYPASS AND PRIMARY TEMPERATURES CALCULATED FROM THE MODEL OF Re=21,000 RUN

Row No.	$T_{b,i}$ ^0F	$T_{p,i}$ ^0F	$T_{b,o}$ ^0F	$T_{p,o}$ ^0F
4	102.0	105.0	102.0	145.0
5	108.8	129.2	108.8	161.2
6	117.8	140.2	117.8	168.1
7	127.5	145.5	127.5	171.4
8	135.9	151.6	135.9	175.3
9	143.5	157.6	143.5	179.0
10	150.4	163.0	150.4	182.4
11	156.6	168.0	156.6	185.5
12	162.1	172.5	162.1	188.4
14	167.2	176.6	167.2	190.9
15	171.8	180.2	171.8	180.2

TABLE 8

BYPASS AND PRIMARY TEMPERATURE CALCULATED FROM THE MODEL OF Re=31,000 RUN

Row No.	Uniform m_b and m_p				Non-uniform m_b and m_p			
	$T_{b,i}$	$T_{p,i}$	$T_{b,o}$	$T_{p,o}$	$T_{b,i}$	$T_{p,i}$	$T_{b,o}$	$T_{p,o}$
0	106.0	106.0	106.0	132.4	106.0	106.0	106.0	128.8
1	107.2	130.0	107.2	151.5	109.3	126.3	109.3	148.8
2	110.5	144.8	110.5	163.2	112.3	142.8	112.3	161.8
3	116.0	152.1	116.0	168.9	117.5	151.3	117.5	168.4
4	123.1	154.5	123.1	170.9	124.3	154.5	124.3	171.0
5	131.0	155.1	131.0	171.6	132.0	155.4	132.0	171.9
6	138.3	156.9	138.3	173.2	139.1	157.4	139.1	173.6
7	145.1	159.5	145.1	175.0	145.8	160.0	145.8	175.5
8	151.1	162.8	151.1	177.4	151.8	163.3	151.8	177.8
9	156.4	166.7	156.4	180.2	157.0	167.2	157.0	180.6
10	161.2	170.5	161.2	183.0	161.8	171.0	161.8	183.3
11	165.6	174.1	165.6	185.6	166.1	174.5	166.1	185.9
12	169.7	177.4	169.7	188.0	170.1	177.8	170.1	188.3
13	173.3	180.5	173.3	190.2	173.8	180.8	173.8	190.4
14	176.7	183.3	176.7	192.2	177.1	183.6	177.1	192.4
15	179.9	185.9	179.9	185.9	180.2	186.2	180.2	186.2

Note: All the units are ^{0}F.

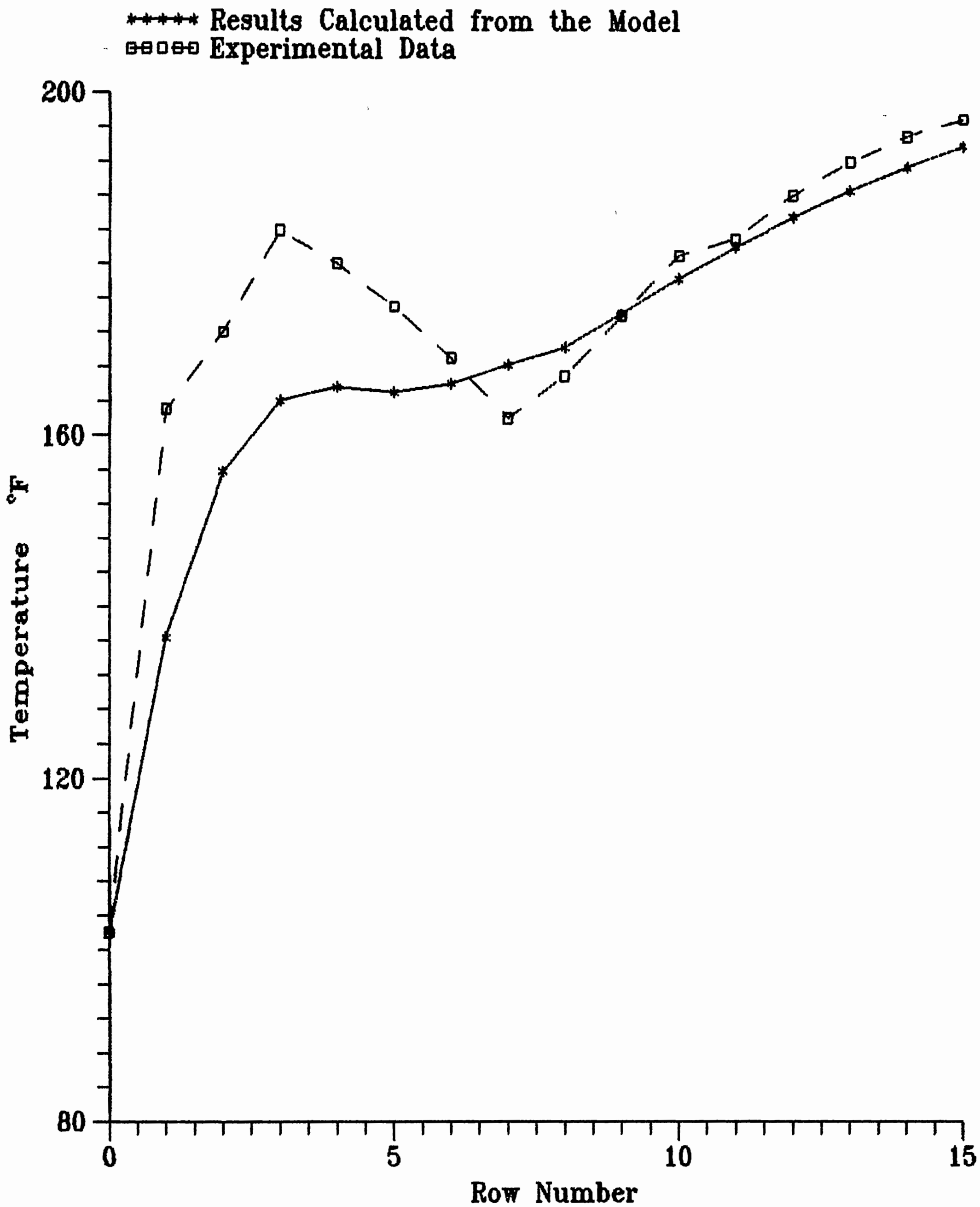

Figure 11. Primary Flow Temperatures for Re=18,000 Run with Uniform Primary Flow Rate

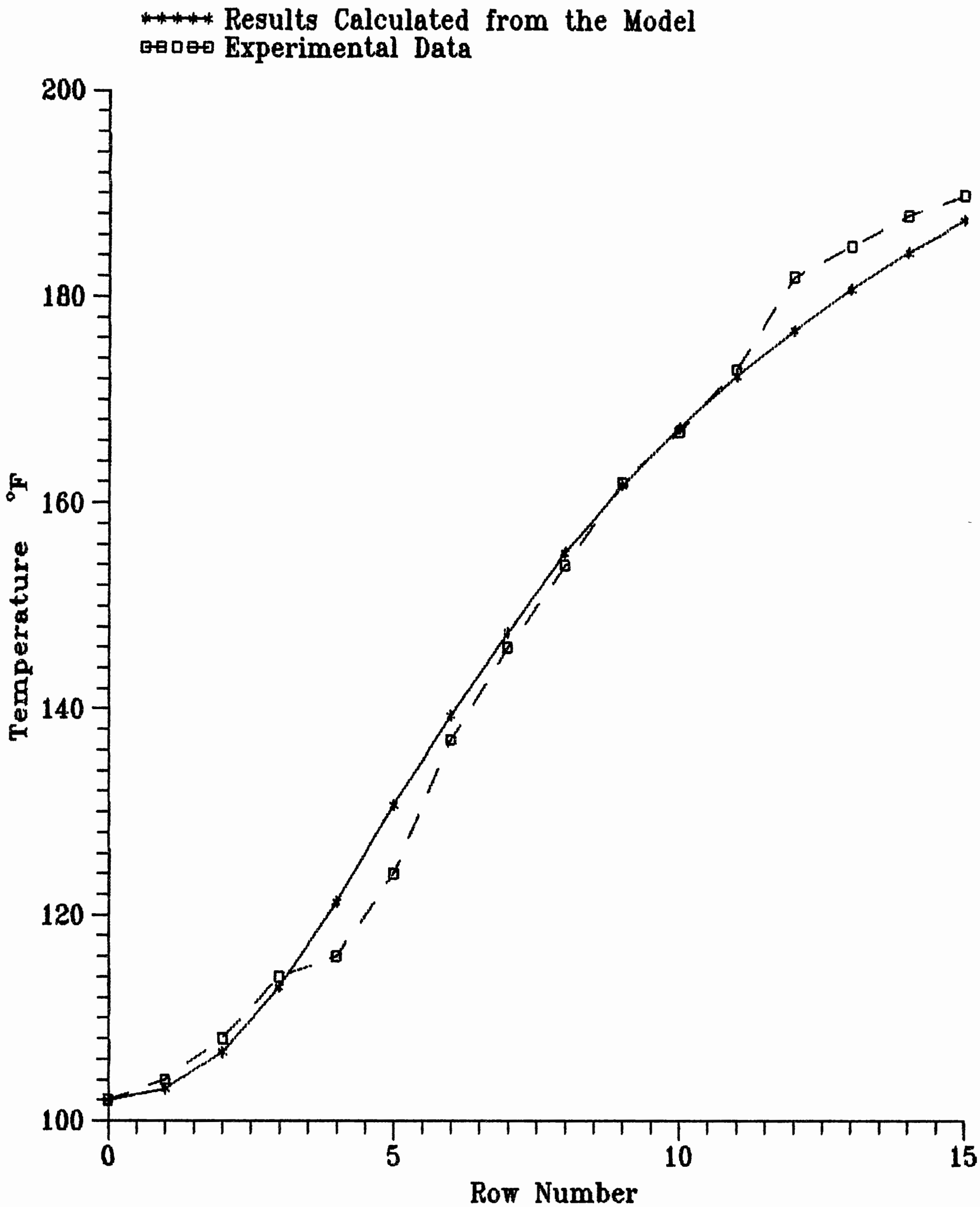

Figure 12. Bypass Flow Temperatures for Re=18,000 Run with Uniform Primary Flow Rate

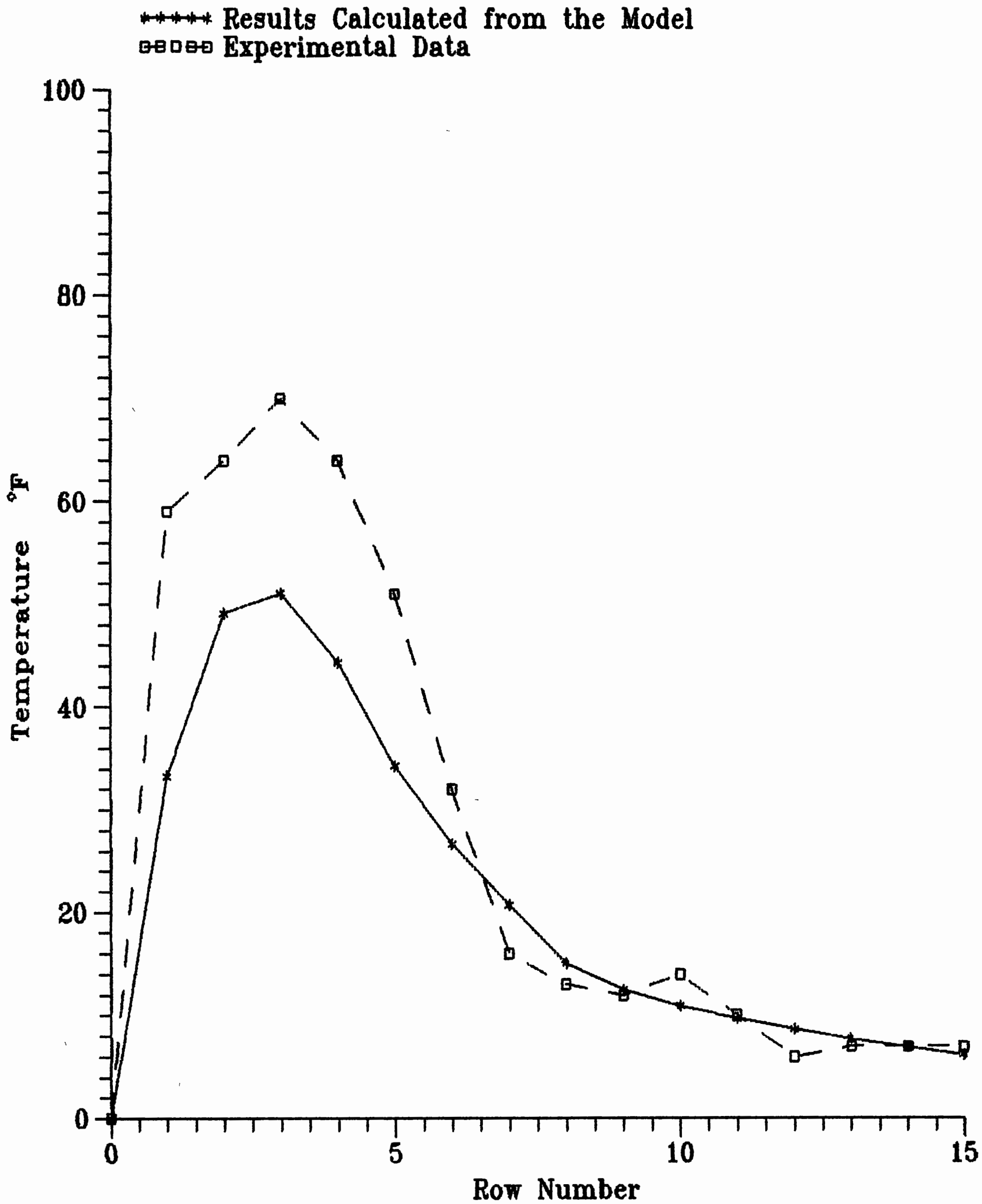

Figure 13. Temperature Difference between Primary and Bypass Flow at Re=18,000 Run with Uniform Primary Flow Rate

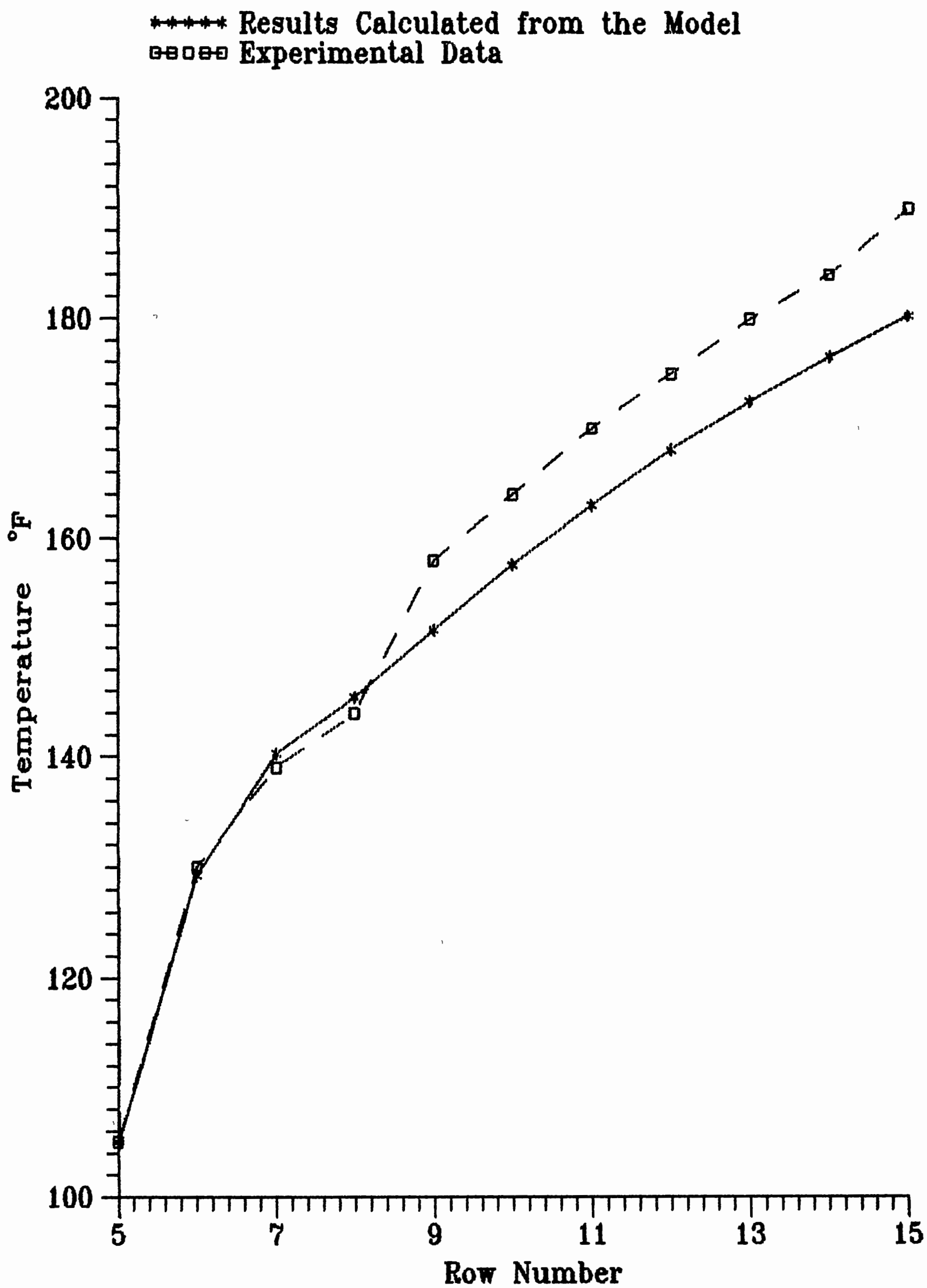

Figure 14. Primary Flow Temperatures for Re=21,000 Run

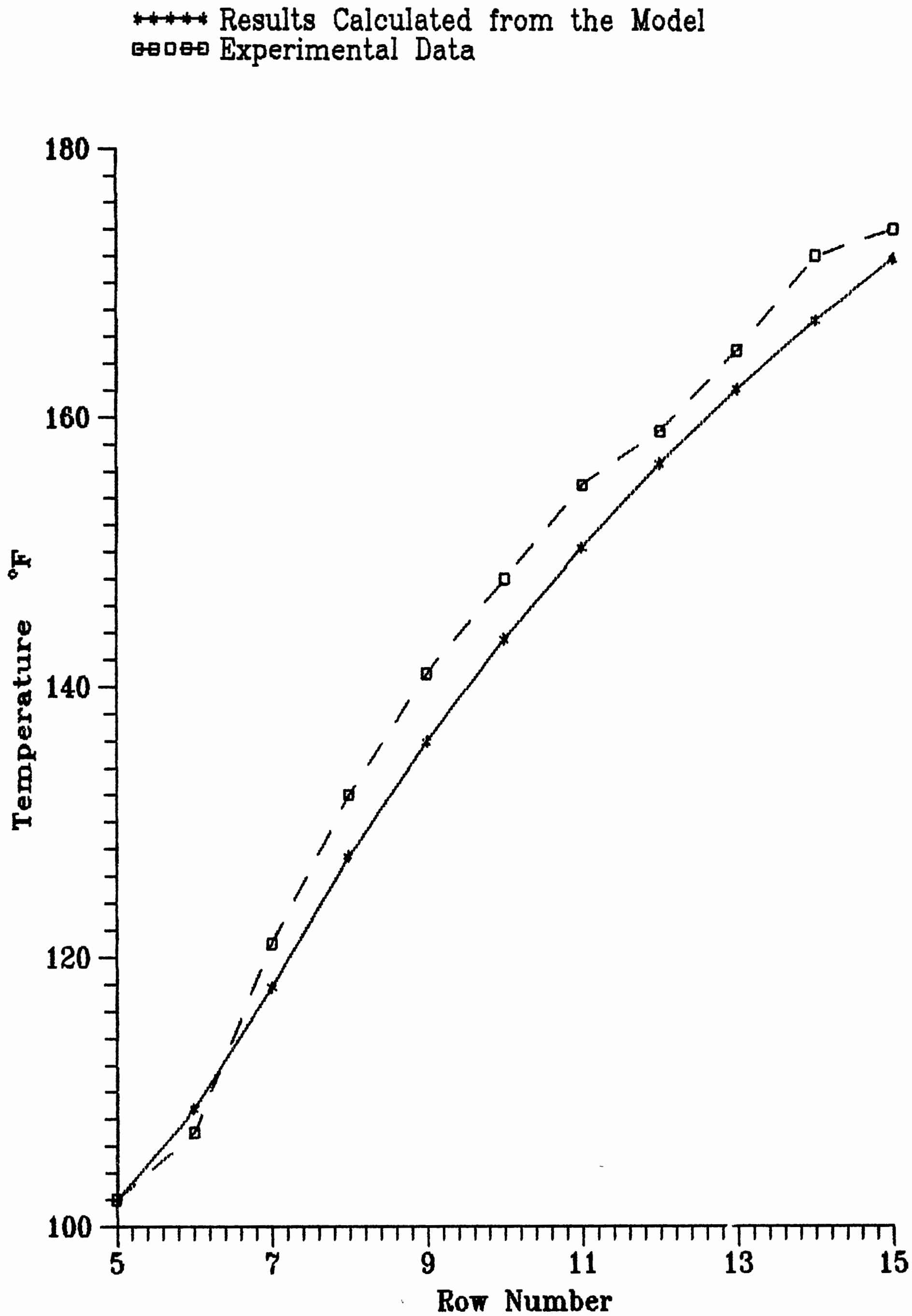

Figure 15. Bypass Flow Temperatures for Re=21,000 Run

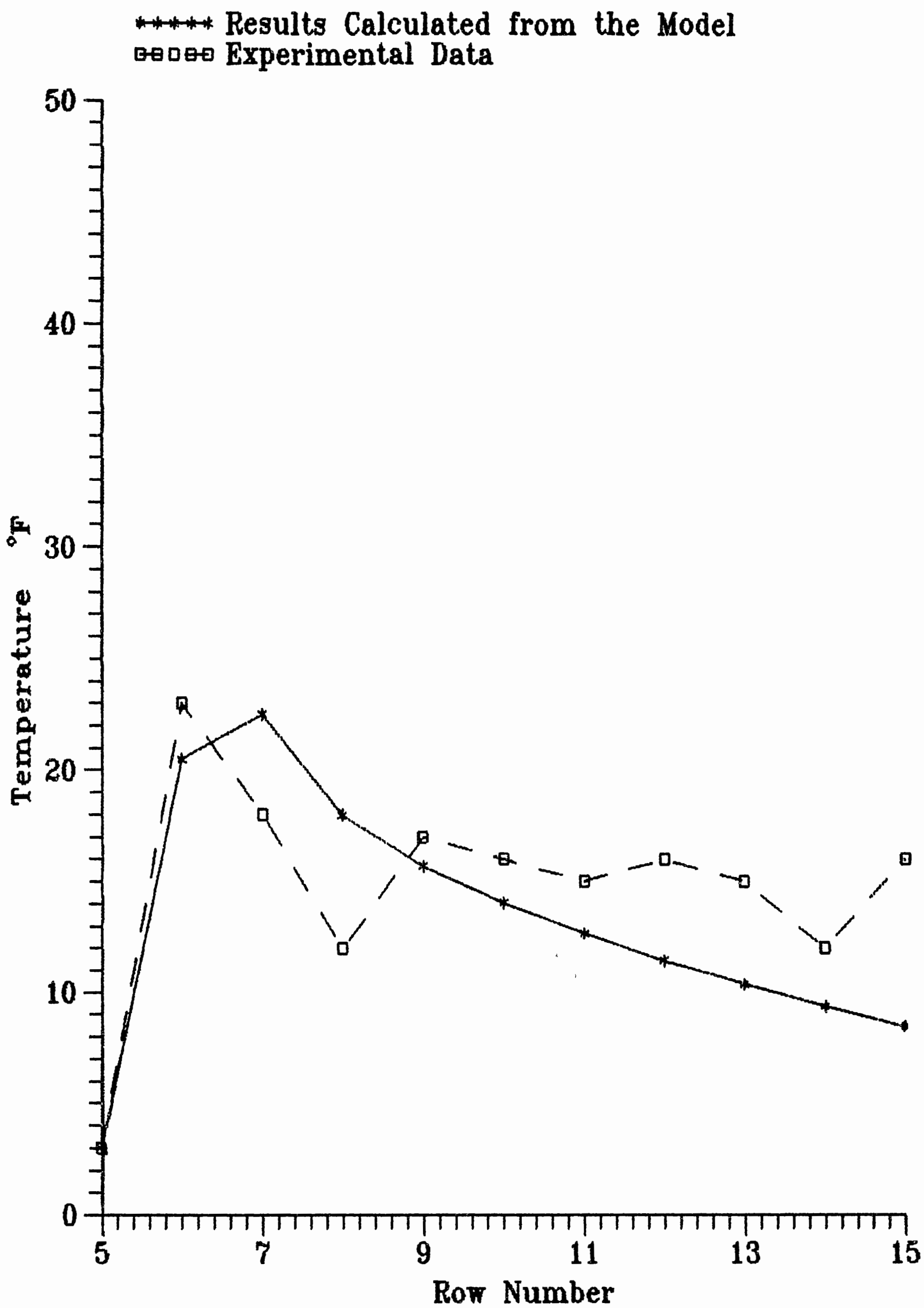

Figure 16. Temperature Difference between Primary and Bypass Flow ar Re=21,000 Run

After the primary flow temperature reaches a maximum point,the flow comes into the transition region, where the primary flow temperature decreases for a few rows. At the same time, the bypass flow temperature increases steadily, and the temperature difference between the two streams decreases quickly. When the temperature difference becomes very small (about 10 ^{0}F), the flow is in what I defined as the fully developed region. In this part, the primary flow temperature increases monotonically along with the bypass flow temperature, and the temperature difference becomes steady.

The above phenomena can be explained by the physical principles of the model. When the flow first enters the tube bank and the primary flow temperature is low, the temperature driving force is large. Thus, the primary flow is quickly heated. At the same time, the flow has not been fully developed, so the interchange flow rate is small, and there is only a small amount of heat been transferred from the primary flow to the bypass flow by exchanging mass. Hence, in the entrance region, the primary flow temperature increases quickly, because it gets much more heat from the tube surface than it loses to the bypass flow. The bypass flow temperature increases slowly because of the small interchange flow rate. When the flow enters the transition region, the primary flow has already been heated close to the saturation temperature of the condensing steam, and the driving force between surface and primary stream becomes small. On the other hand, the interchange flow rate increases, and the bypass flow temperature is still low. So here the primary flow loses heat to the bypass flow much faster than before, and receives from the tube side much slower than in the entrance region. This causes the bypass flow temperature to increase rapidly, but the primary flow temperature increases very slowly or even decreases in this region. After the flow field is developed, the temperature difference between the two streams is small, so the primary flow receives and loses almost the same amount of heat. Thus, in this region, both the primary temperature and the bypass temperature increase steadily, and the temperature difference remains almost the same.

From the Figures, we can also find that the calculated bypass flow temperature profiles fit the experimental data well throughout the tube bank, but the primary flow temperature and the temperature difference profiles only fit the experimental data in the deep tube bank. For the Re=18,000 and Re=31,000 runs, in the shallow tube bank, primary flow temperatures predicted by the model are much lower than the experimental values especially for the first two tube rows. This causes the predicted temperature differences to be much larger than the experimental data.

For the Re=21,000 run, for which only the deep tube bank rows are thermally active, all of the predicted profiles fit the experimental data well. One possible explanation of this phenomena is that the primary flow temperature defined in the model is the average temperature of the whole primary flow at the given tube row, but the experimental data may only reflect the temperature behind the center of the tube. From the Weierman et al. (1975) temperature profiles (Figure 8) behind the 2nd and 4th tube rows, we can see that strong temperature differences within the primary flow exist, while the temperature is much more uniform behind the 7th tube row. So, if the probe was inserted right behind the center point of the tube, the measured primary flow temperature would be higher than the average primary flow temperature among the first several tube rows. For the deep tube bank, since the temperature distribution is uniform, the average primary flow temperature is close to the temperature behind the center point of the tube. Another possible reason is that the assumptions of the primary flow heat transfer coefficients and interchange flow rates, though reasonable, are not actual values. And, the questionable quality of Rabas and Huber's experimental data may also contribute to the inconsistency between experimental data and those calculated from the model.

The estimations of the primary flow heat transfer coefficients are within reasonable ranges. The heat transfer coefficients were checked by the Briggs and Young (1963) correlation for staggered fin tube banks and by accounting for the validity of the LMTD reduction procedure. The heat transfer coefficients obtained from the three methods are listed in Table 9. One sample calculation for the Re=18,000 run is given in Appendix B. From the table, we find that the ratio of h_c from the LMTD procedure to h_{cp} from the model varies from 0.54 to 0.73 for the Re=18,000 Run, from 0.62 to 0.86 for the Re=31,000 Run, and is about 0.83 for the Re=21,000 Run. These values are within the range of inline/staggered heat transfer coefficient ratios that other investigators found. The ratio for the lower Reynolds number (Re=18,000) is smaller then that for the higher Reynolds number (Re=31,000). Also, the deep tube bank (Re=21,000) has a higher ratio. Bell and Kegler (1978) found that the real heat transfer coefficient (as predicted by their model) is close to the value predicted for the staggered array.

From Table 9, we can see that the values from Briggs and Young's correlation are lower than those from the model, especially for the deep tube bank. Consider how Briggs and Young obtain their correlation. The correlation is based on experimental data from a staggered tube bank with six tube rows. From the literature review, we know that even the staggered tube bank has a row number effect. So their correlation may not fit the deep tube bank. Notice that for Re=21,000 run, which only has the deep tubes heated, the heat transfer coefficients obtained from the Briggs and Young correlation are even lower than those from the LMTD method. Also, we find that differences between h_c from the

TABLE 9

HEAT TTRANSFER COEFFICIENTS FROM DIFFERENT METHODS

Method		Re=18,000		Re=21,000		Re=31,000	
		h_c	U_0	h_c	U_0	h_c	U_0
LMTD		8.12	5.40	13.7	7.6	13.1	7.4
This Model	Row 1	11.0	6.63			15.3	8.08
	Row 7	15.0	7.99	16.5	8.44	20.9	9.59
Briggs and Young (1963) Correlation		9.48	6.05	10.5	6.42	13.7	7.6

Note: All the units are Btu/(hr-ft^2-^{0}F).

correlation and h_{cp} assumed for first tube row are within 15 percent.

Since there are so many uncertainties, and also because of the above reasons, we can say that the estimation of heat transfer coefficients is reasonable. Also, the estimated heat transfer coefficients for the three runs are related by $h_{cp} \propto M^{0.6}$. The consistency between the computational results and experimental results of all the three runs shows that the estimation is reasonable.

The estimation of the interchange flow rates is also within the reasonable range. The estimated interchange flow rates range from 2 percent of the total flow at the first tube row to about 14 percent of the total flow rate at the deep tube bank. These values are close to those Bell and Kegler (1978) found from their model.

One interesting note is that changing the bypass and primary flow rate ratio does not affect the results too much. From Table 6 and 8, we see that the two different estimations of the bypass and primary flow rates for the first tube row (with the remaining tube bank having same primary flow rate) gave close results.

The model can also be used to explain Zhang and Chen's (1991) study of inline tube banks with a gap. If there is a gap existing behind one tube row, there should be more interchange flow at the gap, thus decreasing the primary flow temperature and increasing the driving force. Hence, more heat is transferred from the wall to the primary flow.

Thus, the heat transfer has been enhanced as shown by the experimental data of Zhang and Chen.

CHAPTER VI

CONCLUSIONS AND RECOMMENDATIONS

The model presented in this thesis attempts to explain the row number effects on the inline banks of finned tubes. From the model and the data in the literature, we reach the following conclusions:

1. There is a strong bypass flow between the fin tips existing in inline finned tube banks.
2. The flow bypass is the main factor that causes the row number effect on the apparent heat transfer coefficient in inline finned tube banks.
3. The interchange flow rate increases from row to row in a shallow tube bank.
4. Because the interchange flow rate between the primary and bypass flows changes from row to row, several tube rows are required to fully develop the flow.
5. The real heat transfer coefficient for the primary flow increases from row to row in a shallow tube bank.
6. The shallow inline tube bank results in poor heat transfer.
7. Although the data used to verify the model are of poor quality, and in some ways are incomplete, they fit the model well enough. The computational results show that the model

does predict the observed row number effect on heat transfer in inline tube banks at least qualitatively.

Though this model is not complete enough to be used in design now, I believe that with more and better experimental results the model can be generalized and used in design. Moreover, the model can be used as a guide when designing a heat exchanger with an inline finned tube bank.

BIBLIOGRAPHY

Ackerman, J.W. and Brunsvold, A.D. "Heat Transfer and Draft Loss Performance of Extended Surface Tube Banks," Journal of Heat Transfer, vol. 94 :215-220 (1970)

Aoki, T. and Taborek, J. "Survey and Evaluation of Heat Transfer and Pressure Drop Correlations for Ideal Finned Tube Banks With Staggered Tube Layouts," HTRI Report No. ESG-4 (1978)

Bell, K.J. and Kegler, W.M. "Analysis of Bypass Flow Effects in Tube Banks and Heat Exchangers," AIChE Symp. Ser., no. 174 vol. 74 :47-52 (1978)

Briggs, D.E. and Young, E.H. "Convective Heat Transfer and Pressure Drop of Air Flowing Across Triangular Pitch Banks of Finned Tubes," CEP Symp. Ser., no. 41, vol. 59 :1-10 (1963)

Brauer, H. "Compact Heat Exchangers," Chemical and Process Engineering, vol. 45 no. 8 :451-460 (1964)

Carnavos, T.C. "Heat Transfer and Pressure Loss Performance of Griscom-Russell Special Small K-Fin Helically Finned Tubes," Rept. AECU 3970, U.S. Department of Commerce Clearing House (1958)

Eckels, P.W. and Rabas, T.J. "Heat Transfer and Pressure Drop Performance of Finned Tube Bundles," Journal of Heat Transfer, vol. 107 :205-213 (1985)

Gianolio, E. and Cuti. F. 'Heat Transfer Coefficients and Pressure Drop for Air Coolers With Different Numbers of Rows Under Induced and Forced Draft', Heat Transfer Engineering, vol. 3, no. 1 :38-47 (1981)

Hashizume K., (1981) 'Heat Transfer and Pressure Drop Characteristics of Finned Tubes in Cross Flow', Heat Transfer Engineering, vol. 3, no. 2 :15-20 (1981)

Kays, W.M.; London, A.L. and Lo, R.K. "Heat Transfer and Friction Characteristics for Gas Flow Normal to Tube Banks ---- Use of a Transient Technique," Trans. ASME, vol. 76, no. 3 :387-396 (1954)

Kays, W.M. and London, A.L. "Compact Heat Exchangers," 3rd Edition, McGraw-Hill Book Co., New York (1984)

Kegler, W.H. "Effect of Flow Bypass on Heat Exchanger Thermal Performance", MS Thesis, Oklahoma State University (1974)

Kern, D.Q. and Kraus, A.D. "Extended Surface Heat Transfer," McGraw-Hill Book Co., New York (1972)

Pierson, L. "Experimental Investigations of the Influence of Tube Arrangement on Heat Transfer and Flow Resistance in Cross-flow Tube Banks," Trans. ASME, vol. 59 :563-572 (1937)

Rabas, T.J. and Eckels, P.W. "Heat Transfer and Pressure Drop Performance of Segmented Extended Surface Tube Bundles," ASME paper 75-HT-45 (1975)

Rabas, T.J. and Eckels, P.W. "The Effect of a Gap Between Layers on the Heat Transfer and Pressure Drop Performance of Low-Finned Tube Bank," Advances in Enhanced Heat Transfer, ASME HTD vol.43 :11-14 (1985)

Rabas, T.J. and Eckels, P.W. "Effectiveness of Enhancement Devices for Three Row Inline Serrated Finned Tube Banks," ASME paper 84-HT-96 (1984)

Rabas, T.J. and Huber, F.V. "Row Number Effects on the Heat Transfer Performance of In-Line Finned Tube Banks," Heat Transfer Engineering, vol. 10, no. 4 :19-29 (1989)

Webb, R.L. "Air-Side Heat Transfer in Finned Tube Heat Exchangers," Heat Transfer Engineering, vol.1, no.3 :33-49 (1980)

Weierman, C.; Taborek, J. and Marner, W.J. "Comparison of Inline and Staggered Banks of Tubes With Segmented Fins," AIChE Symp. Ser., vol.74, no.174 :39-46 (1978)

Weierman, C.; Yarden, A.; and Taborek, J. "Heat Transfer and Pressure Drop on An Inline Tube Bank With Segmented Fins," HTRI Report No. ESG-P2 (1975)

Weierman, C.; and Taborek, J. "Comparison of the Performance of Inline and Staggered Banks of Tubes with Segmented Fins," HTRI Report No.ESG-8 (1978)

Weierman, C.; and Taborek, J. "HTRI Extended Surface Data Book," (1978) Zhang, Y.; and Chen, Z. "The Effect of Gap Between Layers on the Heat Transfer Performance of Aligned Tube Banks," (It will be published on Heat Transfer Engineering.) (1992)

Zukauskas, A.A., (1972) 'Heat Transfer From Tubes in Cross Flow', Advances in Heat Transfer, vol.8, Academic Press, New York, pp 154-155 (1972)

APPENDIXES

APPENDIX A

TEMPERATURE PROFILES

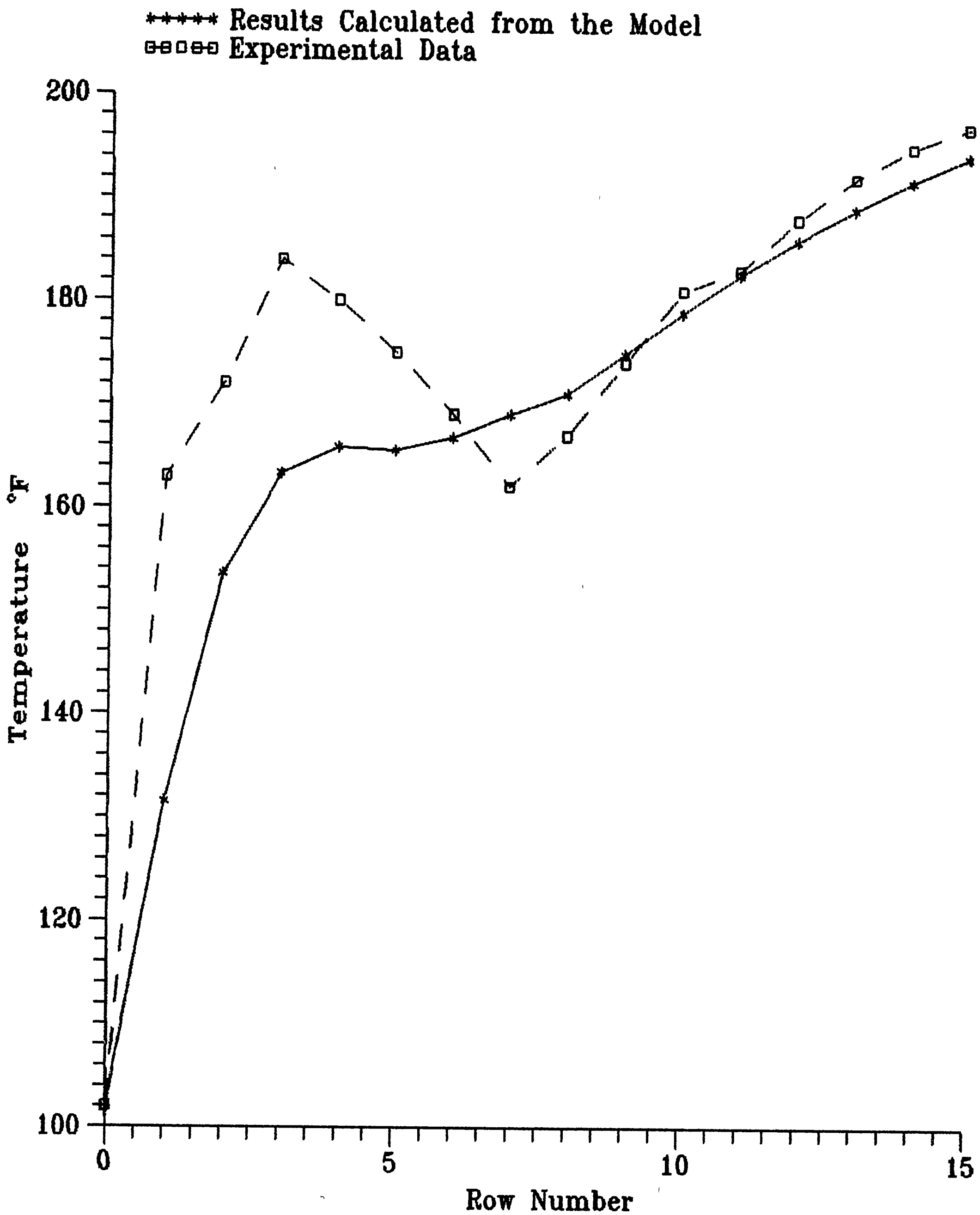

Figure 17. Primary Flow Temperatures for Re=18,000 Run with Non-Uniform Primary Flow Rate

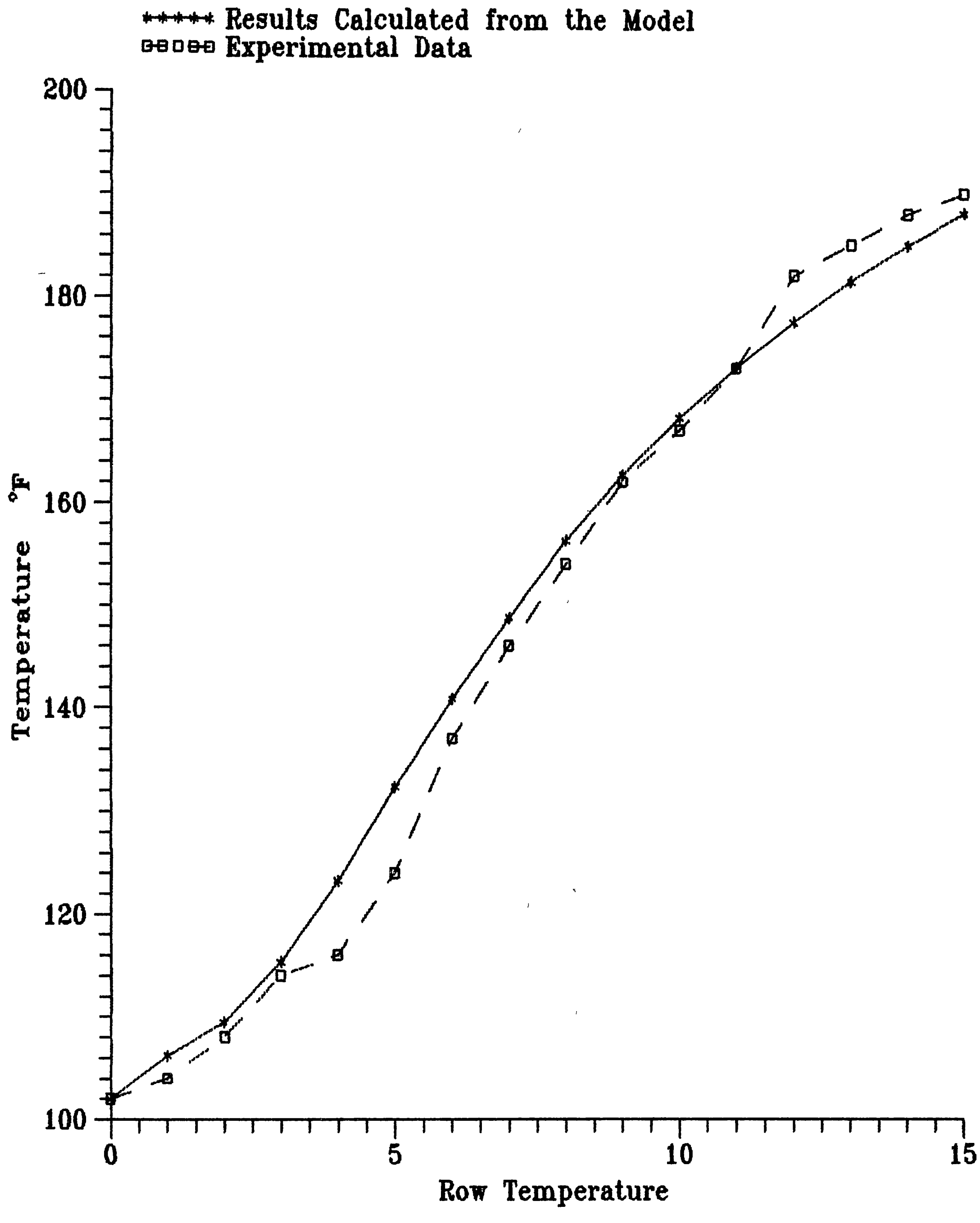

Figure 18. Bypass Flow Temperatures for Re=18,000 Run with Non-uniform Primary Flow Rate

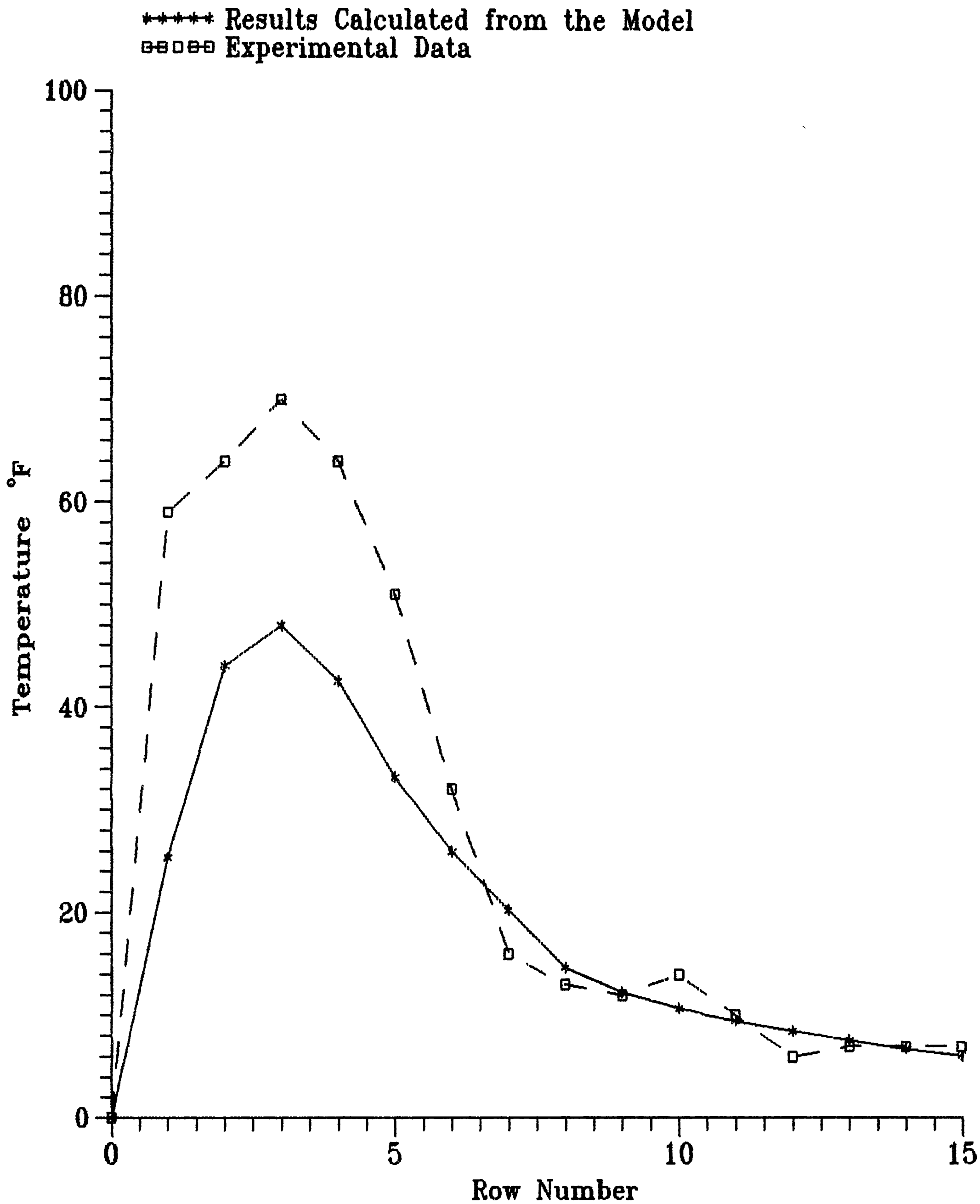

Figure 19. Temperature Difference between Primary and Bypass Flow Rate ar Re=18,000 Run with Non-uniform Primary Flow Rate

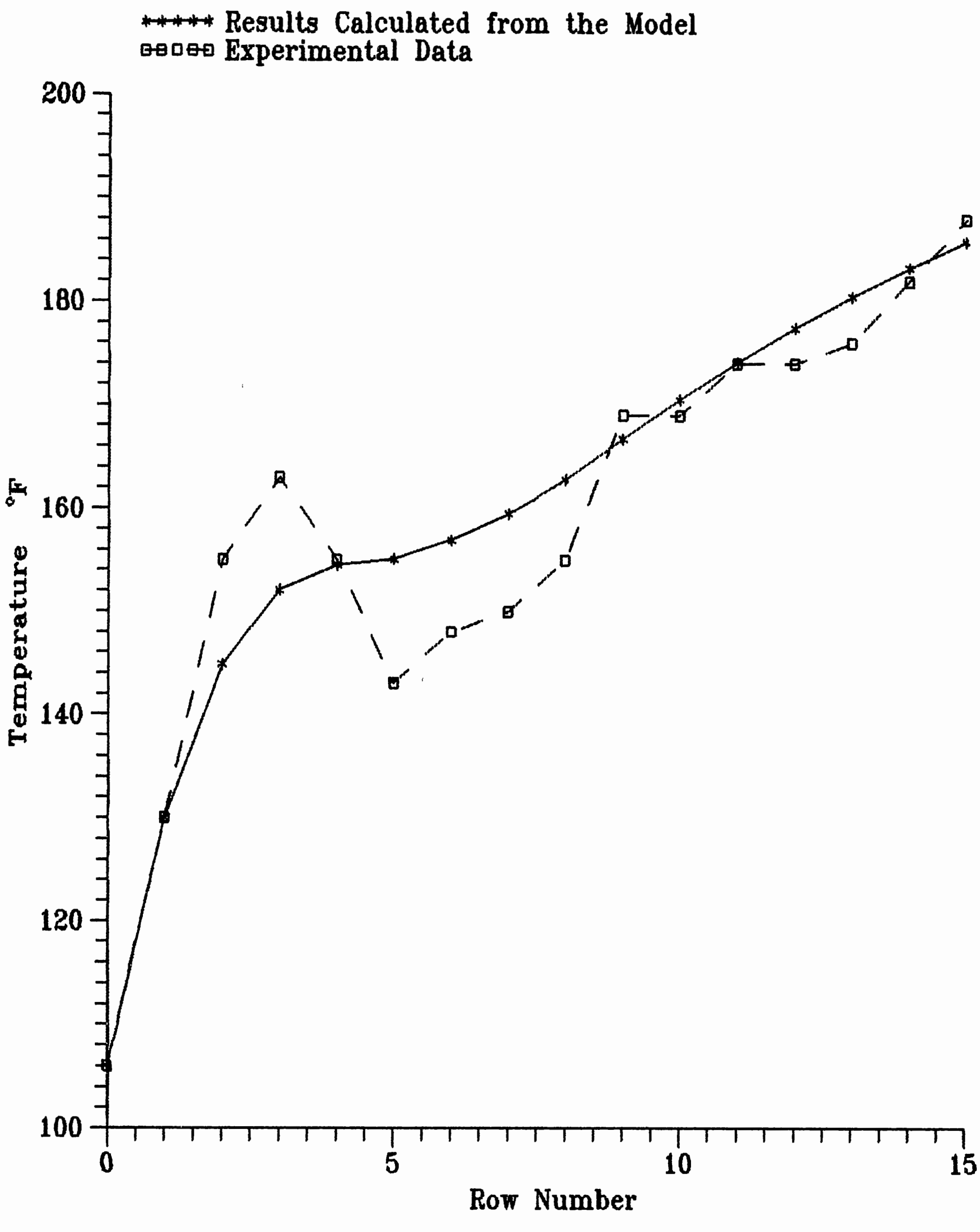

Figure 20. Primary Flow Temperatures for Re=31,000 Run with Uniform Primary Flow Rate

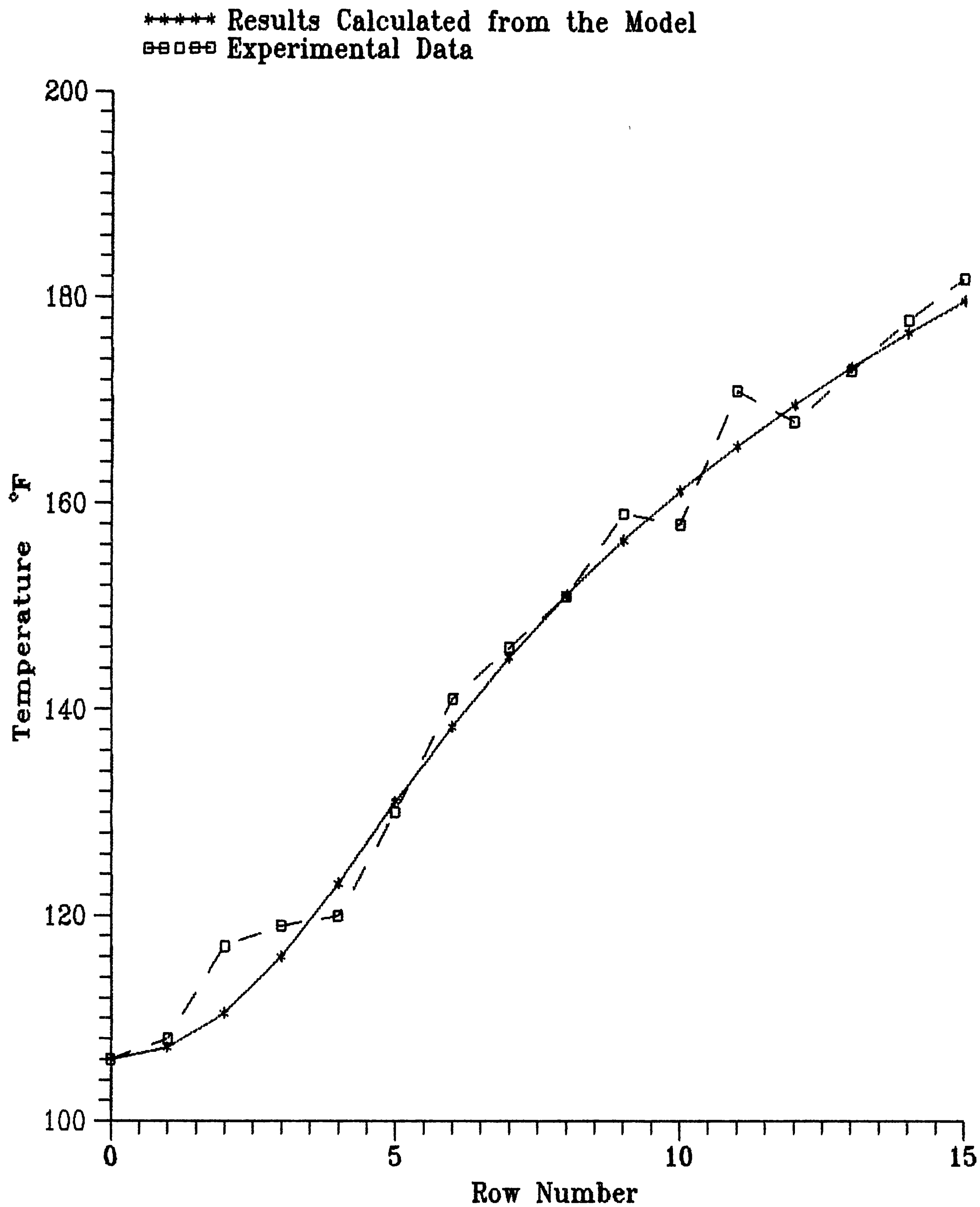

Figure 21. Bypass Flow Temperatures for Re=31,000 Run with Uniform Primary Flow Rate

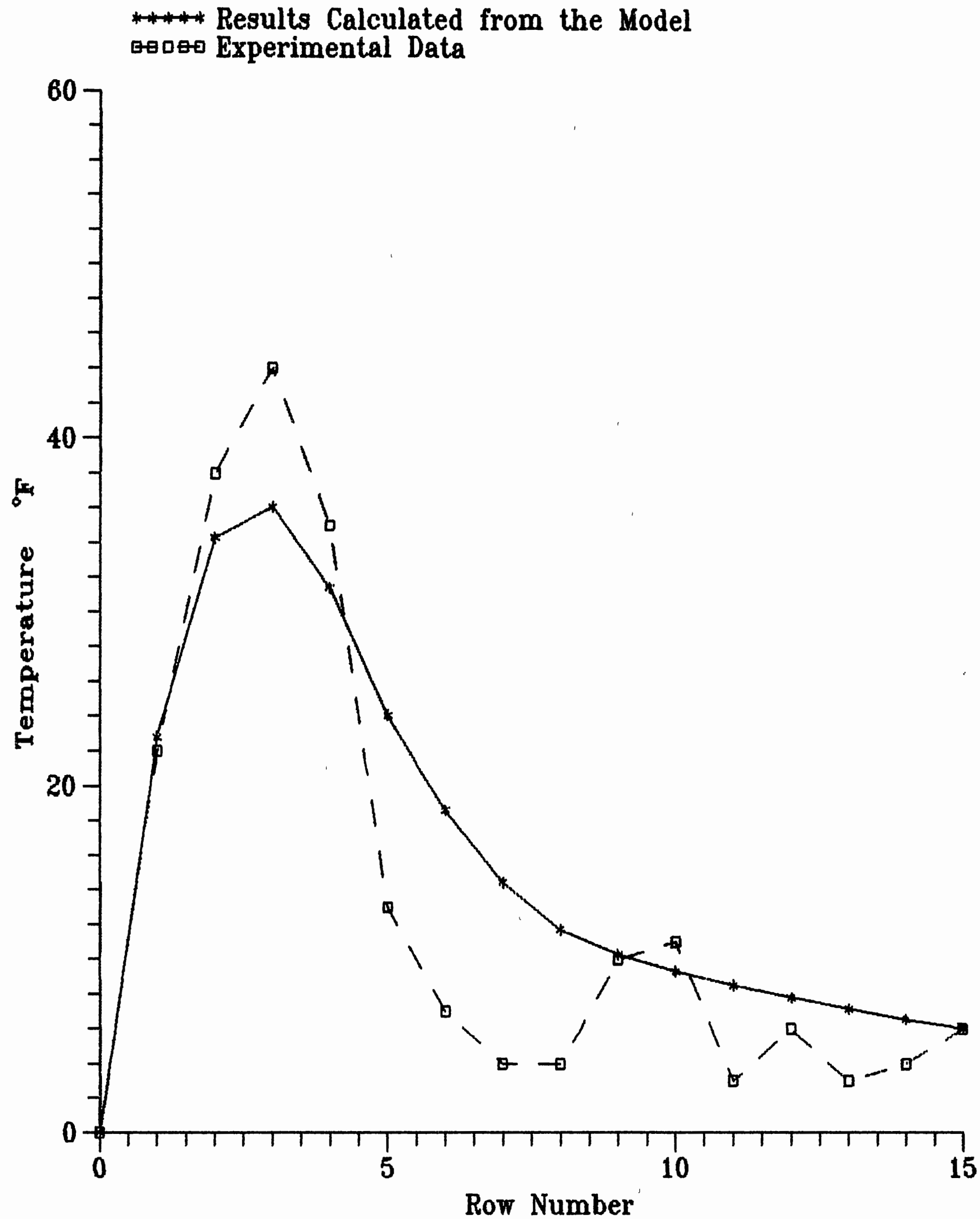

Figure 22. Temperature Difference between Primary and Bypass Flow at Re=31,000 Run with Uniform Primary Flow Rate

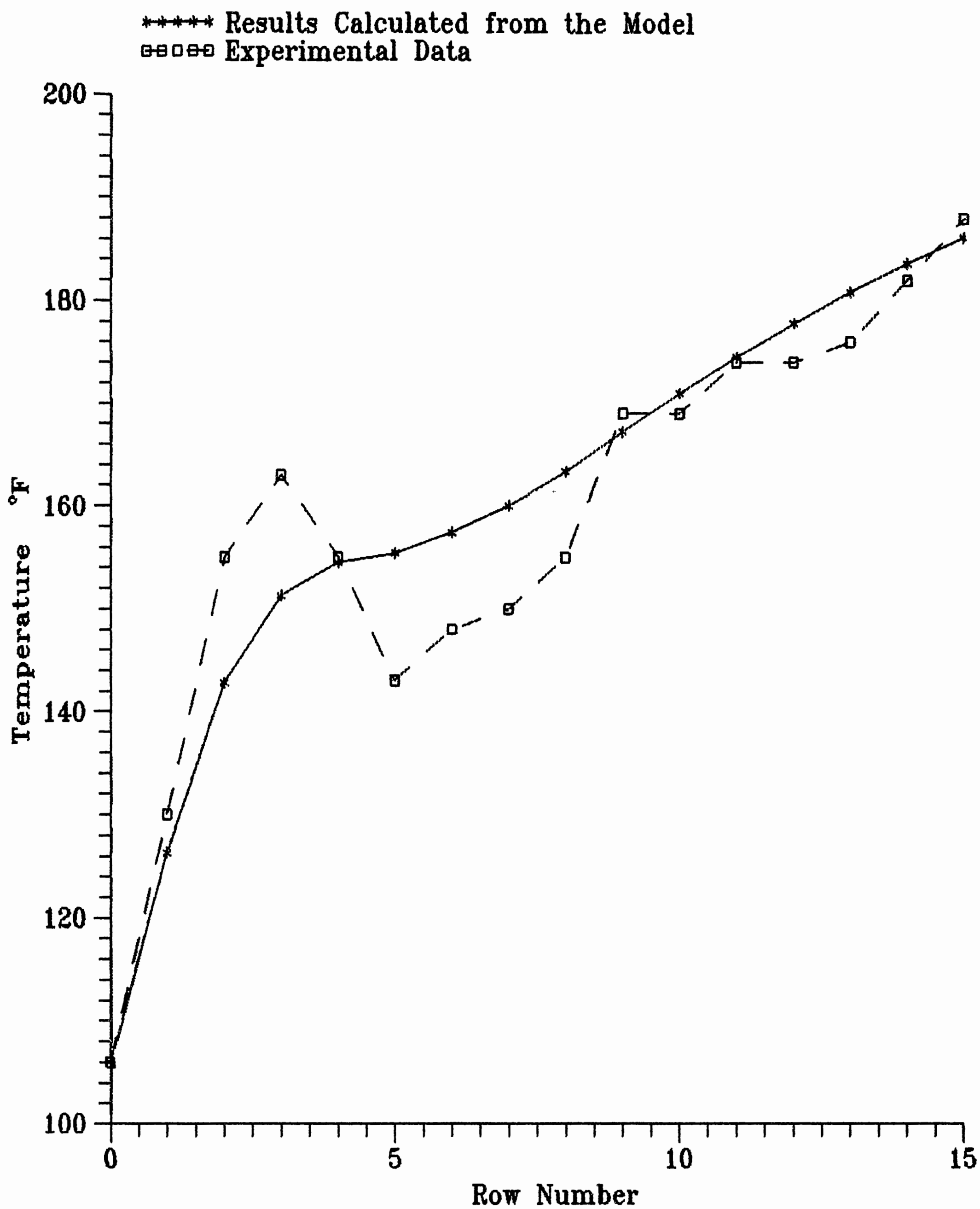

Figure 23. Primary Flow Temperatures for Re=31,000 Run with Non-Uniform Primary Flow Rate

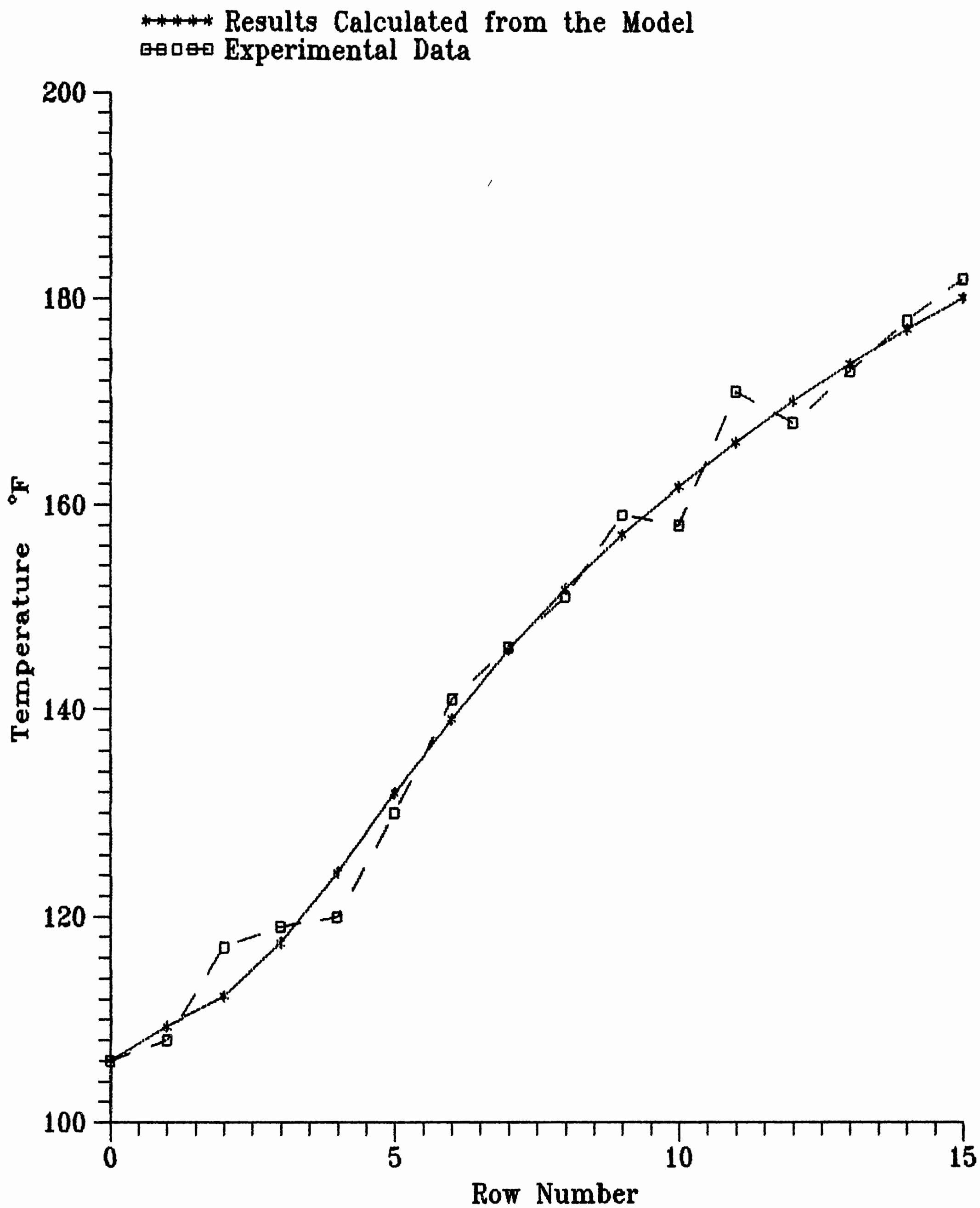

Figure 24. Bypass Flow Temperatures for Re=31,000 Run with Non-Uniform Primary Flow Rate

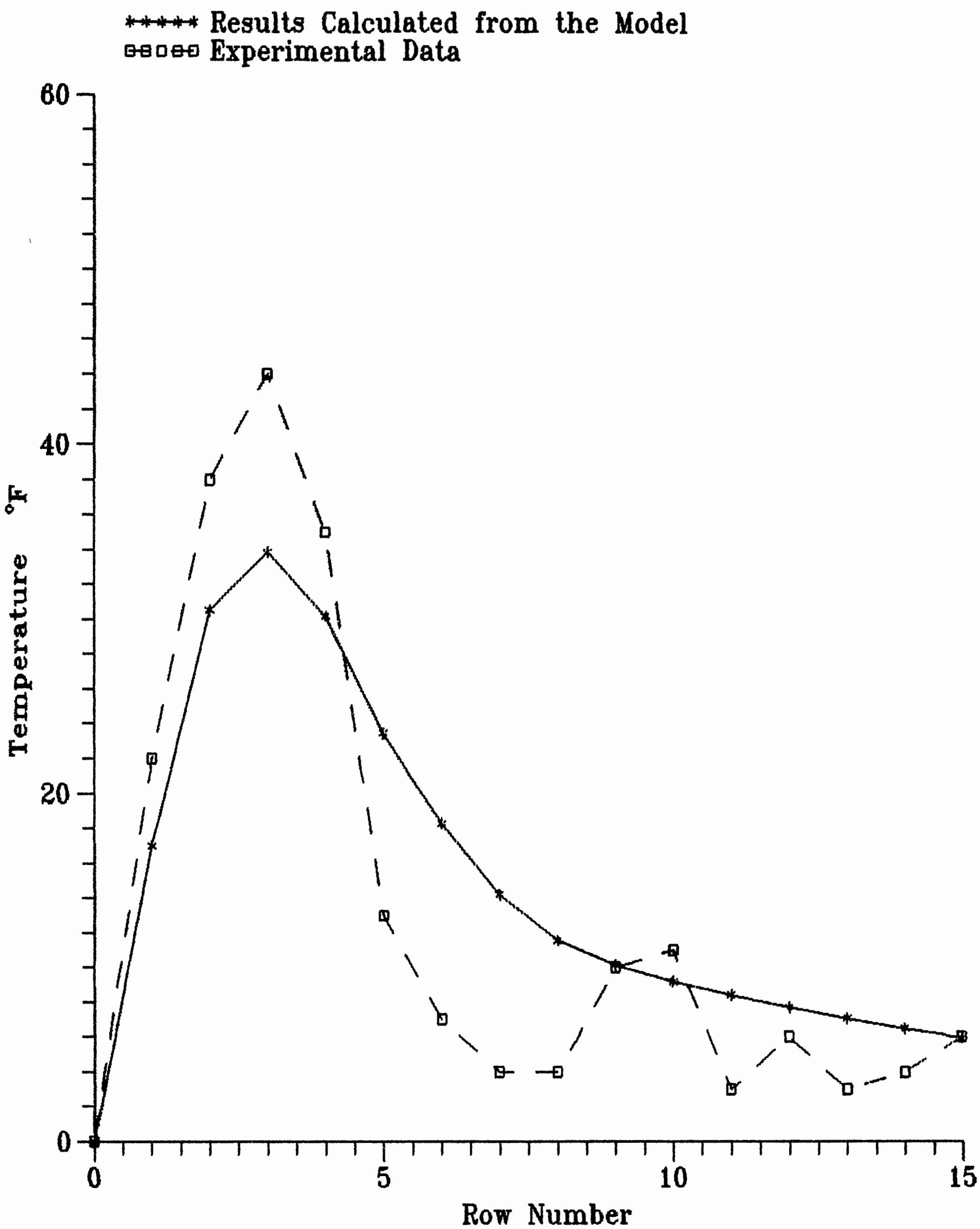

Figure 25. Temperature Difference between Primary and bypass Flow at Re =31,000 Run with Non-Uniform Primary Flow Rate

APPENDIX B

CALCULATION OF HEAT TRANSFER COEFFICIENT USING LMTD METHOD AND BRIGGS AND YOUNG'S (1963) CORRELATION

In this appendix, the Re=18,000 run was again selected to do the sample calculation.

1. LMTD Method

The temperatures from the experimental data at the 15th tube row were selected as the outlet temperatures.

For Re=18,000,

$$T_{b,15} = 190\ ^0F \quad ; \quad T_{p,15} = 197\ ^0F$$

assume

$$m_b = 3600\ lbm/hr \quad ; \quad m_p = 1800\ lbm/hr \tag{1}$$

and

$$\overline{T}_{out} = \frac{T_b m_b + T_p m_p}{M} \tag{46}$$

$$= \frac{190*3600+197*1800}{5400}$$

$$= 192°F.$$

Hence

$$Q = c_p M(\overline{T}_{out} - T_{in}) \tag{47}$$

$$= 0.24*5400*(192-102)$$

$$= 1.17*10^5\ Btu/hr$$

and

$$LMTD = \frac{\overline{T}_{out} - T_{in}}{\ln(\frac{T_s - T_{in}}{T_s - \overline{T}_{out}})} \tag{48}$$

$$= \frac{192-102}{\ln(\frac{215-102}{215-192})}$$

$$= 56.5^oF$$

From

$$Q = U_o * A * LMTD, \tag{49}$$

we can have

$$U_o = \frac{Q}{A * LMTD}$$

$$= \frac{1.17*10^5}{382.5*56.5}$$

$$= 5.4\ Btu/(hr\text{-}ft^2\text{-}^oF).$$

Also, we have

$$h_a = [\frac{1}{U_o} - R_{th}]^{-1} \tag{45}$$

where

$$R_{th} = 0.0174\ (hr\text{-}ft\text{-}^0F)/Btu.$$

Hence:

$$h_a = [\frac{1}{5.4} - 0.174]^{-1} = 5.96 Btu/(hr\text{-}ft^2\text{-}^oF).$$

In order to get the h_c, we first need to calculate the fin efficiency:

$$\Omega = \frac{\tanh(z l_e)}{z l_e} \qquad (5)$$

where

$$z = \sqrt{\frac{2h_c}{k t_e}} \quad ; \quad t_e = \frac{t_f w_s}{t_t + w_s} \quad ; \quad and \ \ l_e = l \qquad (6)$$

where

t_f = 0.004 ft

w_s = 0.013 ft

l_e = 0.083 ft

k = 30.3 Btu/(hr-ft^2-^{0}F)

Assume h_c = 8.2 Btu/(hr-ft^2-^{0}F).

Hence:

Ω = 0.724.

We have

$$h_c = \frac{h_a}{1-(1-\Omega)\frac{(A_f)_o}{A_o}} \qquad (44)$$

where

$(A_f)_0$ = 6.13 ft^2/ft ; A_0 = 6.36 Btu/(hr-ft^2-^{0}F)

Hence:

$$h_c = \frac{5.96}{1-(1-0.724)*\frac{6.13}{6.36}}$$

$$= 8.12\ Btu/(hr\text{-}ft^2\text{-}^oF)$$

If we assume

m_b = 3618 lbm/hr ; m_p =1782 lbm/hr

then

$$\overline{T}_{out} = \frac{3618*190+1782*197}{5400} = 192^oF$$

The average outlet temperature was almost the same as before. The change of bypass and primary flow rates assumed will not affect the h_c found from the LMTD method.

2. Briggs and Young's Correlation

The Briggs and Young (1963) correlation is

$$\frac{h_c d_r}{k} = 0.134\left(\frac{d_r \rho V_{max}}{\mu}\right)^{0.68} Pr^{\frac{1}{3}}\left(\frac{H}{s}\right)^{-0.2}\left(\frac{Y}{s}\right)^{-0.12} \qquad (51)$$

From it, we can get

$$h_c = 0.134\frac{k}{d_r}\left(\frac{d_r \rho V_{max}}{\mu}\right)^{0.68} Pr^{\frac{1}{3}}\left(\frac{H}{s}\right)^{-0.2}\left(\frac{Y}{s}\right)^{-0.12} \qquad (52)$$

where

Dr = 0.104 ft

k = 17*10 Btu/(hr-ft^2-^{0}F) (at air temperature 150 ^{0}F)

ρ = 6.5*10 lbm/ft^{-2} (at air temperature 150 ^{0}F)

V_{max}= 36.2 ft

μ = 13.6*10 lbm/sec ft

H = l =0.083 ft (Fin Height)

s = s_f - t_f = 0.006 ft (Space between fins)

Y = t = 0.004 ft (Mean fin thickness)

Pr = 0.70.

Hence:

$$h_c = 0.134*\frac{17*10^{-3}}{0.104}*(\frac{0.104*6.5*10^{-}2*36.2}{13.6*10^{-6}})^{0.68}$$

$$*(0.70)^{(\frac{1}{3})}*(\frac{0.083}{0.006})^{-0.2}*(\frac{0.004}{0.006})^{-0.12}$$

$$= 9.48\ Btu/(hr\text{-}ft^2\text{-}^oF).$$

From the calculation before, we have t_e = 0.0031 ft.

So, we can get

$$z = \frac{\sqrt{2*h_c}}{k*t_e}$$

$$= \sqrt{\frac{2*9.48}{30.3*0.0031}}$$

$$= 14.4\ ft^{-1},$$

and

$$\Omega = \frac{\tanh(zl_e)}{zl_e}$$

$$= \frac{\tanh(14.2*0.083)}{14.2*0.083}$$

$$=0.696.$$

Hence:

$$h_a = h_c[1-(1-\Omega)\frac{(A_f)_o}{A_o}]$$

$$= 9.48*[1-(1-0.696)]*\frac{6.13}{6.36}$$

$$= 6.70 \quad Btu/(hr\text{-}ft^2\text{-}^oF).$$

Hence:

$$U_o = \frac{1}{\frac{1}{h_a} + R_{th}}$$

$$= \frac{1}{\frac{1}{6.70}+0.0174}$$

$$= 6.05 \quad Btu/(hr\text{-}ft^2\text{-}^oF)$$

APPENDIX C

COMPUTER PROGRAM LISTING

AND FLOW CHARTS

NOMENCLATURE FOR COMPUTER PROGRAM

A: Total effective heat transfer area per row; ft^2/row

AF: Finned outside area per unit length; ft^2/ft

AHA: Actual film heat transfer coefficient (based on the total outside effective heat transfer area); Btu/hr-ft^2-^{0}F

AHC: Film heat transfer coefficient calculated assuming 100 % fin efficiency (based on the total outside effective heat transfer area); Btu/(hr-ft^2-^{0}F)

AO: Total outside surface area per unit length; ft^2/ft

CON: Thermal conductivity; Btu/(hr-ft^2-^{0}F)

EL: Fin height; ft

ERR1: Error of calculated primary stream temperature to experimental data; ^{0}F

ERR2: Error of calculated bypass stream temperature to experimental data; ^{0}F

HI: Tube side heat transfer coefficient; Btu/(hr-ft^2-^{0}F)

N: Number of tube rows; dimensionless

OME: Fin efficiency; dimensionless

R: Thermal resistance (tube side convective resistance and the tube wall conductive resistance); (hr-ft^2-^{0}F)/Btu

TBI: Calculated bypass stream temperature approaching a given tube row; ^{0}F

TBIE: Experimental bypass stream temperature approaching a given tube row; ^{0}F

TBO: Calculated bypass stream temperature existing at a given tube row; ^{0}F

TE: Effective fin thickness; ft

TF: Fin thickness; ft

TPI: Calculated primary stream temperature approaching a given tube row; ^0F

TPO: Calculated primary stream temperature existing at a given tube row; ^0F

TPIE: Experimental primary stream temperature approaching a given tube row; ^0F

TF: Fin thickness; ft

TS: Tube side stream temperature; ^0F

U: Overall heat transfer coefficient for primary stream (based total outside surface area); Btu/(hr-ft^2-^{0}F)

WB: Bypass stream flow rate; lbm/hr

WBE: Flow rate of interchange stream from bypass stream to primary stream divided by total stream flow rate; dimensionless

WP: Primary stream flow rate; lbm/hr

WPE: Flow rate of interchange stream from primary stream to bypass stream divided by total stream flow rate; dimensionless

WS: Fin segment width; ft

WT: Total stream flow rate; lbm/hr

Z: Fin efficiency parameter; ft^{-1}

MAIN PROGRAM

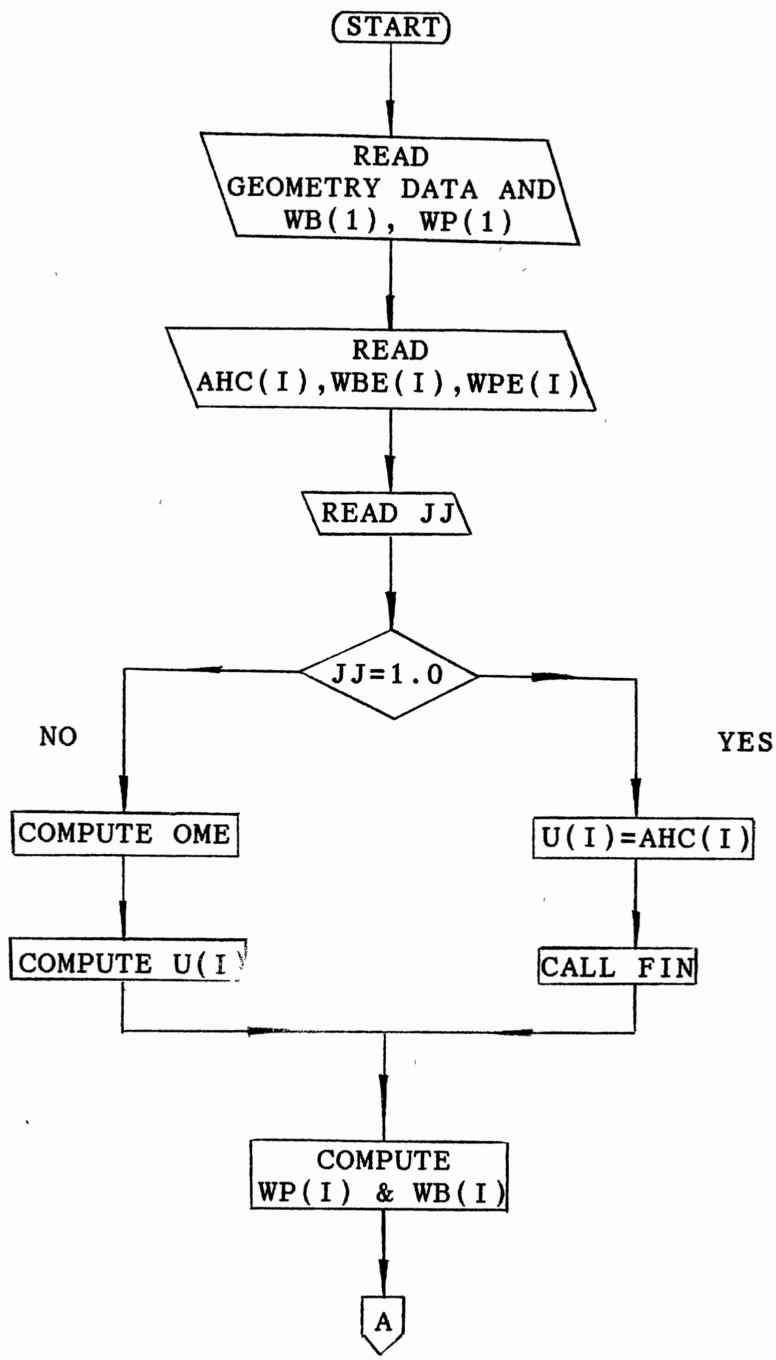

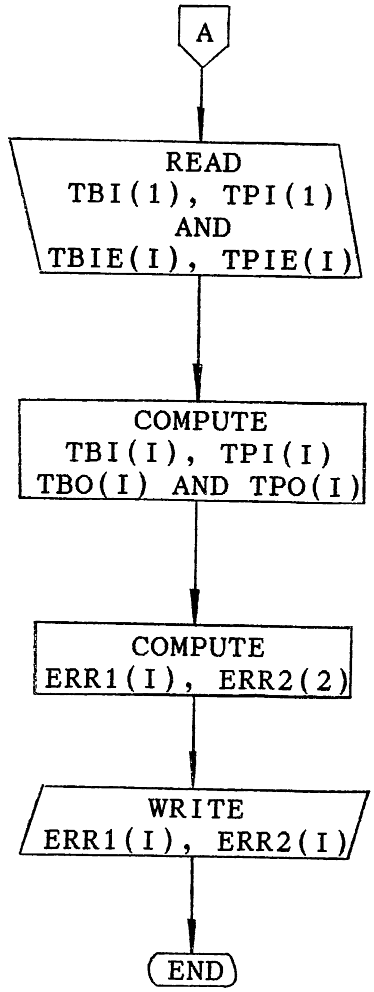
A
READ
TBI(1), TPI(1)
AND
TBIE(I), TPIE(I)
COMPUTE
TBI(I), TPI(I)
TBO(I) AND TPO(I)
COMPUTE
ERR1(I), ERR2(2)
WRITE
ERR1(I), ERR2(I)
END

SUBROUTINE FIN

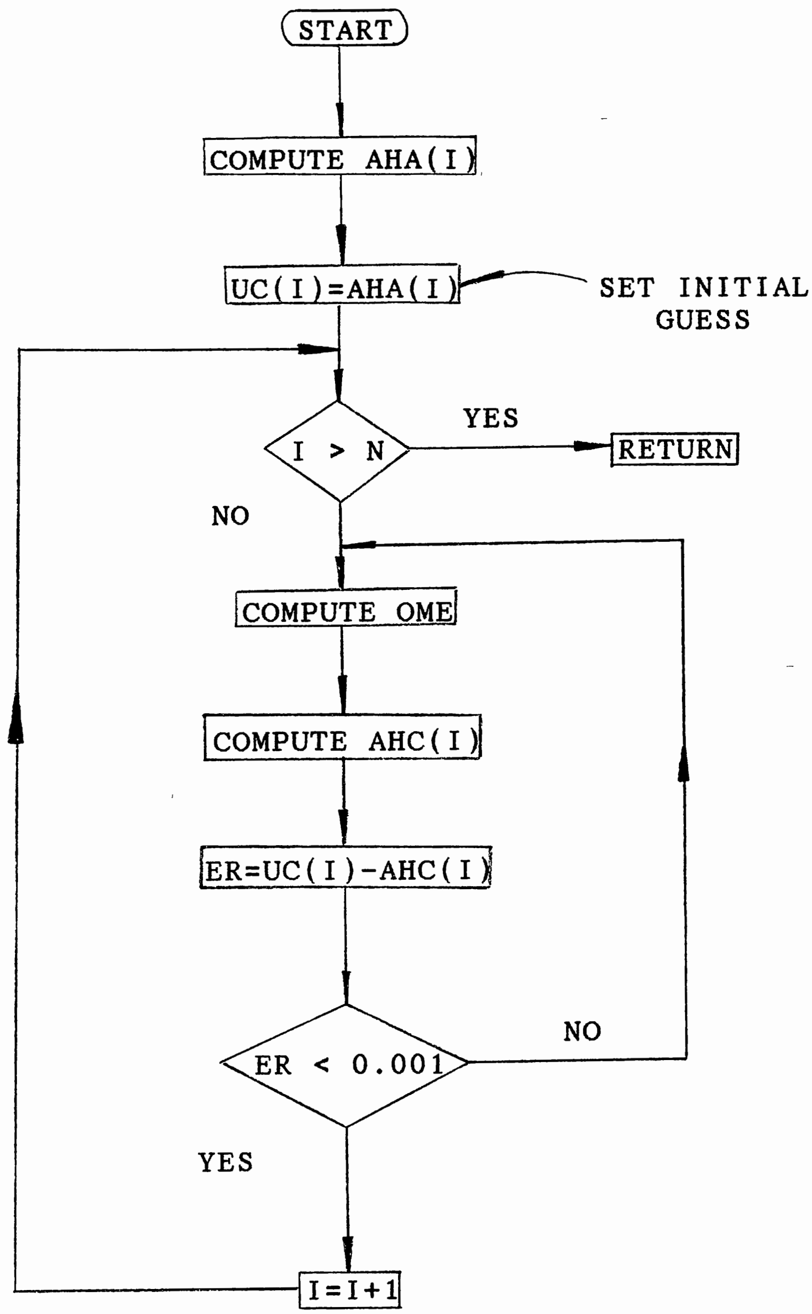

```
C    THIS PROGRAM IS DEVELOPED TO CALCULATE THE      C
C  BYPASS AND PRIMARY TEMPERATURE USING THE NEW      C
C  MODEL AND COMPARE THEM WITH THE EXPERIMENTAL      C
C  DATA.                                             C
CCCCCCCCCCCCCCCCCCCCCCCCCCCCCCCCCCCCCCCCCCCCCCCCCCCCC
C
C
C
C     JJ: =1     OVERALL HEAT TRAN COEF KNOW
C         =0     AIR SIDE HEAT TRAN COEF WITH 100%
C                  FIN EFFICIENCY KNOWN
C
C
C MAIN PROGRAM
       DIMENSION WBE(20),WPE(20)
       DIMENSION TPIE(20),TBIE(20),ERR1(20),ERR2(20)
       DIMENSION WB(20),WP(20)
C
       COMMON /C1/ TBI(20),TBO(20),TPI(20),TPO(20)
       COMMON /C2/ AHC(20),AHA(20),U(20)
       COMMON /C3/ EL,TF,WS,CON,AF,AO,R,N
C
       OPEN(9,FILE='IN.DAT',STATUS='OLD')
       OPEN(8,FILE='OUT.DAT',STATUS='UNKNOWN')
C
C---------INPUT TUBE GEOMETRY, AIR FLOW RATE,
C             AND TUBE SIDE TEMPERATURE
C
       READ(9,*)TF,WS,EL,AF,AO,CON,R
       READ(9,*)TS,A,N
       READ(9,*)WB(1),WP(1)
       WRITE(8,*)'TS=',TS,'WP(1)=',WP(1),'WB(1)=',WB(1)
       WRITE(8,*)'A=',A,'N=',N
C
C-----READ HEAT TRANS COEF, INTER CHANGE FLOW RATE
C
       DO I=1,N
         READ(9,*)AHC(I),WBE(I),WPE(I)
       ENDDO
C
C------READ JJ FOR KNOW HC OR U
C
       READ(9,*)JJ
C
       IF(JJ.EQ.1)THEN
C
C------CALCULATE HC
C
           DO I=1,N
             U(I)=AHC(I)
           ENDDO
C
           CALL FIN
C
```

```
      ELSE
C
C------CALCULATE U
C
          TE=TF*WS/(TF+WS)
          DO I=1,N
            Z=(2.*AHC(I)/(CON*TE))**0.5
            OME=(EXP(Z*EL)-EXP(-Z*EL))
     *         /(EXP(Z*EL)+EXP(-Z*EL))
            OME=OME/(Z*EL)
            AHA(I)=AHC(I)*(1.-(1.-OME)*AF/AO)
          ENDDO
C
          DO I=1,N
            U(I)=1./((1./AHA(I))+R)
          ENDDO
C
      ENDIF
C
C----------CALAULATE BYPASS AND PRIMARY FLOW RATE
C
      WT=WP(1)+WB(1)
      DO I=2,N+1
        WP(I)=WP(I-1)+(WBE(I-1)-WPE(I-1))*WT
        WB(I)=WB(I-1)+(WPE(I-1)-WBE(I-1))*WT
      ENDDO
C
C-----------INPUT EXPERIMENTAL DATA
C
      READ(9,*)TBI(1),TPI(1)
      DO I=1,N+1
         READ(9,*)TBIE(I),TPIE(I)
      ENDDO
C
      WRITE(*,*)' I    HC(I)    U(I)       WBE(I)
     *       WPE(I)'
      WRITE(8,*)' I    HC(I)    U(I)       WBE(I)
     *       WPE(I)'
      DO I=1,N
        WRITE(*,1000)I,AHC(I),U(I),WBE(I),WPE(I)
        WRITE(8,1000)I,AHC(I),U(I),WBE(I),WPE(I)
      ENDDO
C
C----------CALCULATE BYPASS AND PRIMARY TEMPERATURE
C
        DO I=1,N+1
          TBO(I)=TBI(I)
          B=EXP(U(I)*A/(WP(I)*0.24))
          TPO(I)=((B-1.)*TS+TPI(I))/B
          TBI(I+1)=(TBO(I)*WB(I)-TBO(I)*WBE(I)*WT+
     *        TPO(I)*WPE(I)*WT)/WB(I+1)
          TPI(I+1)=(TPO(I)*WP(I)-TPO(I)*WPE(I)*WT+
     *        TBO(I)*WBE(I)*WT)/WP(I+1)
        ENDDO
```

```
C
C-----------CALAULATE AND OUTPUR ERROR
C
        DO I=1,N+1
          ERR1(I)=TPI(I)-TPIE(I)
          ERR2(I)=TBI(I)-TBIE(I)
        ENDDO
C
        WRITE(8,*)
        WRITE(*,*)
        WRITE(8,*)
        WRITE(*,*)
        WRITE(8,*)'I  TBI(I)   TPI(I)   TBO(I)   TPO(I)'
        WRITE(*,*)'I  TBI(I)   TPI(I)   TBO(I)   TPO(I)'
        DO I=1,N+1
          WRITE(8,2000)I,TBI(I),TPI(I),TBO(I),TPO(I)
          WRITE(*,2000)I,TBI(I),TPI(I),TBO(I),TPO(I)
        ENDDO
C
        DO I=1,N+1
          WRITE(8,*)I,' ','TPI(I)-TPIE(I)=',ERR1(I),
     *  'TBI(I)-TBIE(I)=',ERR2(I)
          WRITE(*,*)I,' ','TPI(I)-TPIE(I)=',ERR1(I),
     *  'TBI(I)-TBIE(I)=',ERR2(I)
        ENDDO
C
        DO I=1,N+1
        A=ERR1(I)-ERR2(I)
          WRITE(8,*)I,' ','TEMP DIFF ERR=',A
          WRITE(*,*)I,' ','TEMP DIFF ERR=',A
        ENDDO
C
1000    FORMAT(1X,I2,2X,F5.2,3X,F5.2,3X,F8.3,3X,F8.3)
2000    FORMAT(1X,I3,2X,F5.1,4X,F5.1,4X,F5.1,4X,F5.1)
        STOP
        END
```

```
C
C-----------------------------------------------------------C
        SUBROUTINE FIN
C-----------------------------------------------------------C
C
        DIMENSION UC(20)
        COMMON /C1/ TBI(20),TBO(20),TPI(20),TPO(20)
        COMMON /C2/ AHC(20),AHA(20),U(20)
        COMMON /C3/ EL,TF,WS,CON,AF,AO,R,N
C
        DO I=1,N
          AHA(I)=1./((1./U(I))-R)
        ENDDO
C
C-------SET INITIAL GUESS OF AHC(I)
C
        DO I=1,N
          UC(I)=AHA(I)
        ENDDO
C
C-------ITERATION PROCEDURE
C
        TE=TF*WS/(TF+WS)
C
        DO I=1,N
99        Z=(2.*UC(I)/(CON*TE))**0.5
          OME=(EXP(Z*EL)-EXP(-Z*EL))
     *       /(EXP(Z*EL)+EXP(-Z*EL))
          OME=OME/(Z*EL)
          AHC(I)=AHA(I)/(1.-(1.-OME)*AF/AO)
          ER=ABS(UC(I)-AHC(I))
C
          IF(ER.GT.0.01) THEN
            UC(I)=AHC(I)
            GOTO 99
          ENDIF
        ENDDO
C
        RETURN
        END
```

VITA

XIYU YANG

Candidate for the Degree of

Master of Science

Thesis: ROW NUMBER EFFECT ON HEAT TRANSFER IN INLINE BANKS WITH FINNED TUBES

Major Field: Chemical Engineering

Biographical:

Personal Data: Born in Shanghai, People's Republic of China, May 10, 1968, the son of Chengjun Yang and Renji Wang

Education: Graduated from Shixi High School, Shanghai, P.R.China, in July 1986; received the Bachelor of Science degree in Process Equipment from the East China University of Chemical Technology, Shanghai, P.R.China, in July 1990; completed requirements for the Master of Science degree in Chemical Engineering of the Oklahoma State University in July, 1992.

Professional Experience: Graduate Research Assistant, Department of Chemical Engineering, Oklahoma State University, 1990-91.